TÉCNICO LISBOA

Exploring the anticancer properties of colonic metabolites derived from Virgin Olive Oil

Rafaela Sofia Geraldo Pereira

Thesis to obtain the Master of Science Degree in

Biological Engineering

Supervisors: Dra. Ana Teresa de Carvalho Negrão Serra
Prof. Arsénio do Carmo Sales Mendes Fialho

Examination Committee

Chairperson: Professora Maria Margarida Fonseca Rodrigues Diogo
Supervisor: Dra. Ana Teresa de Carvalho Negrão Serra
Member of the committee: Professora Joana Paiva Gomes Miranda

December 2019

I declare that this document is an original work of my own authorship and that it fulfills all the requirements of the Code of Conduct and Good Practices of the Universidade de Lisboa.

Preface

The work presented in this thesis was performed in the Food Functionality and Bioactives laboratory of the Food and Health Division of *iBET – Instituto de Biologia Experimental e Tecnológica* (Oeiras, Portugal), from February to August of 2019. This work was supervised by Dra. Teresa Serra from iBET, within the scope of the curricular course Master Dissertation aiming to obtain the Master Degree in Biological Engineering at Instituto Superior Técnico (Lisbon, Portugal). The thesis was co-supervised at Instituto Superior Técnico by Prof. Arsénio Fialho.

Acknowledgments

Quero expressar o meu agradecimento a todos aqueles que contribuíram direta ou indiretamente na execução desta dissertação de mestrado.

Primeiramente, quero agradecer à Dra. Teresa Serra, a quem posso apelidar não só de orientadora, mas também de mentora por, desde a primeira entrevista, ter confiado em mim e no meu potencial, por ter acompanhado de perto todas as minhas vitórias e desafios e por me ter encorajado a ultrapassar as minhas próprias expectativas. Quero ainda agradecer todos os conhecimentos que me transmitiu e por toda a paciência para esclarecer as dúvidas que tive, quer na fase laboratorial, quer na fase de escrita desta dissertação.

Quero ainda expressar o meu agradecimento à Professora Maria do Rosário Bronze por me ter dado a oportunidade de realizar o meu estágio de dissertação nos laboratórios *Food Functionality and Bioactives* do iBET.

À Dra. Cristina Albuquerque agradeço a oportunidade de desenvolver alguma da parte experimental da minha dissertação nos Laboratórios de Biologia Molecular do Instituto Português de Oncologia de Lisboa Francisco Gentil (IPOLFG) e por toda a preciosa ajuda e disponibilidade demonstrada ao longo deste período. Agradeço ainda à Lucília Pereira por todo o acompanhamento e ajuda disponibilizada.

De seguida, não posso deixar de agradecer aos meus colegas de laboratório do iBET por todos os conselhos e orientação ao longo dos seis meses de estágio. Obrigada Sheila por me teres ajudado a dar os primeiros passos no laboratório, por me teres transmitido tanto conhecimento e por teres ficado noite dentro comigo no laboratório todas as vezes que foram precisas. Obrigada Melanie por me ajudares a manter a calma em alturas mais stressantes e ajudado sempre que precisei. Obrigada Inês, foste a minha companhia nestes seis meses, provavelmente a pessoa que mais de perto acompanhou o dia-a-dia do laboratório. Obrigada ainda ao Martim, ao Baixinho, ao Agostinho, à Ana Bárbara e à Elsa pelos momentos de riso e descontração.

Aos meus Pais atribuo o meu maior e mais profundo agradecimento por me terem acompanhado e apoiado nos melhores e especialmente nos piores momentos, não só destes meses de dissertação como ao longo dos 5 anos de curso.

Por fim, quero agradecer aos meus amigos e família pelos momentos de companheirismo, descontração e paciência.

Abstract

Colorectal cancer (CRC) is among the leading causes of mortality through the world. The Mediterranean diet has shown protective action against CRC due to the intake of different components, being one of the main ones, the virgin olive oil (VOO). Hydroxytyrosol (HT) the most important phenolic compound in VOO, is reported to present several biological activities including anticancer effect. However, the molecular mechanisms underlying the protective action of HT on CRC are still unclear as well as its effect on cancer stem cells subpopulation.

The aim of this thesis was to evaluate the effect hydroxytyrosol and its colonic metabolites, namely phenyl (PA and PPA) in inhibiting proliferation and targeting cancer stemness on a 3D cell model of CRC - HT29 cell spheroids.

Results showed that HT presented the highest antiproliferative effect in both monolayers (EC_{50} = 93.58 µM) and spheroids (EC_{50} = 3938 µM) of HT29 cells. Additionally, HT was the only compound capable of targeting cancer stemness by i) reducing $ALDH^+$ cells (reductions of 16.4% and 39% for 200 µM and 600 µM, respectively) and ii) totally inhibiting colony formation at concentrations above 50 µM. For the same concentrations tested, PA and PPA showed no significant effect. Gene expression analysis revealed that HT at 200 µM slightly reduced the expression of markers related to stemness (*NANOG, OCT4*), Epithelial to Mesenchymal Transition (*VIM*, *TGFβ1*), Sonic Hedgehog Pathway (*GLI1, PTCH1*) and proliferation (*CCNA2)*.

This research work shows great promise in developing new and better ways of tackling colorectal cancer treatment, focusing not only on targeting normal cancer cells, but also cancer stem cells resorting to olive oil bioactive compounds.

Keywords: cancer stem cells, colorectal cancer, hydroxytyrosol, virgin olive oil, 3D cell model

Resumo

O cancro colorrectal encontra-se entre as maiores causas de mortalidade em todo o mundo. A dieta Mediterrânica tem demonstrado ação protetora contra este tipo de cancro devido à ingestão de diversos componentes, sendo um dos principais, o azeite virgem. Hidroxitirosol (HT), o composto fenólico mais importante do azeite virgem, é conhecido por ter várias atividades biológicas, incluindo efeito anticancerígeno. No entanto, os mecanismos moleculares subjacentes à ação protetora do HT no cancro colorrectal continuam pouco claros, assim como o seu efeito na subpopulação de células cancerígenas estaminais.

O objetivo desta tese foi avaliar o efeito do hidroxitirosol e dos seus metabolitos (ácido fenilacético – PA – e ácido fenilpropiónico – PPA) na inibição da proliferação e na modelação das características estaminais do cancro num modelo de cancro colorrectal – esferoides de células HT29.

Os resultados obtidos demonstraram que o HT apresentou o maior efeito antiproliferativo tanto em monocamada (EC_{50} = 93.58 µM) como nos esferoides (EC_{50} = 3938 µM) de células HT29. Adicionalmente, HT foi o único composto capaz de modelar a população de células estaminais cancerígenas ao i) reduzir a população de células $ALDH^+$ (redução de 16.4% e 39% para 200 µM e 600 µM, respetivamente) e ii) totalmente inibir a formação de colónias para concentrações superiores a 50 µM. Para as mesmas concentrações testadas, os compostos PA e PPA não demonstraram efeito significativo. A análise à expressão de genes demonstrou que o HT 200 µM reduziu ligeiramente a expressão de marcadores relacionados com características estaminais (*NANOG,OCT4*) transição epitelial mesenquimal (*VIM, TGFβ1*), *Sonic Hedgehog Pathway* (*GLI1, PTCH1*) e proliferação (*CCNA2*).

Este estudo demonstrou uma enorme promessa no desenvolvimento de novas e melhores maneiras de combater o cancro colorrectal, com foco não só nas células cancerígenas, mas também nas células estaminais cancerígenas recorrendo a compostos do azeite com bioatividade.

Palavras-chave: células estaminais cancerígenas, cancro colorrectal, hidroxitirosol, azeite virgem, modelo celular 3D

List of Contents

List of Figures

List of Tables

List of Abbreviations

Abbreviation	Full Form
2D	Two dimension
3D	Three dimension
5-FU	5-Fluorouracil
APC	Adenomatous polyposis coli
cDNA	Complementary DNA
CFU	Colony Forming Unit
CRC	Colorectal cancer
CSC	Cancer Stem Cell
DEAB	Diethylaminobenzaldehyde
EC_{50}	Half maximal effective concentration
ECM	Extracellular Matrix
EFSA	European Food Safety Authority
EMT	Epithelial to Mesenchymal Transition
FACS	Fluorescence-Activated Cell Sorting analysis
FAP	Familial Adenomatous Polyposis
FBS	Fetal Bovine Serum
HNPCC	Hereditary Nonpolyposis Colorectal Cancer (Lynch Syndrome)
HT	Hydroxytyrosol
JPS	Juvenile Polyposis Syndrome
MTT	reagent (3-(4,5-dimethylthiazol-2-yl)-2,5-diphenyltetrazolium bromide)
PA	Phenylacetic acid
PBS	Phosphate-buffered saline
PPA	Phenylpropionic acid
ROS	Reactive Oxygen Species
RPMI	Roswell Park Memorial Institute
SD	Standard Deviation
SHH	Sonic Hedgehog
TGF	Transforming Growth Factor
VOO	Virgin Olive Oil
WHO	World Health Organization

1. Introduction

1.1. Cancer, its impact and epidemiology

Cancer is a health issue that has taken proportions that approaches an epidemic like state. It is expected to rank as the leading cause of death and the single most important barrier to increasing life expectancy in every country of the world in the 21st century.[1] It is therefore urgent to study this disease and understand its mechanisms of survival and development in order to have a chance at wining the battle against it.

According to studies performed by the World Health Organization (WHO) in 2015, cancer was the first or second leading cause of death before the age of 70 years old in 91 of the 172 countries analyzed, and it takes the 3rd or 4th place in another 22 countries as represented in figure 1.[1] This increase in cancer incidence and mortality reflects both aging worldwide and rapid growth of the population, being this increase also due to the decline in mortality rates of stroke and coronary diseases relative to cancer.[1,2] In emerging economies, the increase of magnitude of this disease accompanies a change in the profile of common cancer types[1].

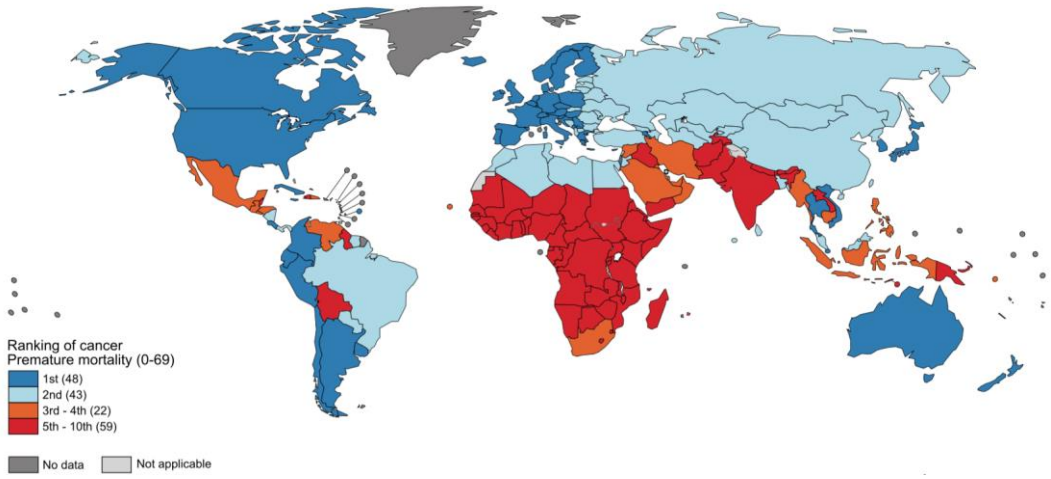

Figure 1 - World map representation of the national ranking of cancer as the cause of death for people under the age of 70 years (2015) - adapted[1]

According to GLOBOCAN 2018, it was estimated that there would be 18.1 million new cases of cancer and 9.6 million cancer related deaths in the world, with Europe representing 23.4% of the total cancer cases and 20.3% of the cancer deaths. [1,3]

In terms of incidence and mortality, lung cancer is the most commonly diagnosed cancer (11.6% of total cases) and also the one that causes the biggest amount of deaths (18.4% of all cancer deaths). Colorectal cancer incidence lays at 10.2% of total cases and poses a mortality of 9.2% of the total cancer deaths.[1,3]

1.2. Colorectal cancer

1.2.1. Incidence and risk factors

Colorectal cancer (CRC) is among the leading causes of mortality and morbidity through the world, representing a major public health problem.[2] This disease incidence varies across racial groups, with the highest percentage of mortality in Blacks, American Indians and Alaska Natives. This discrepancy between races can be explained by environmental factors, delays in the introduction of screening and different management of the disease. Most of these differences are explained by disparities in the socioeconomic status. It was also observed that the incidence rates are higher in individuals of the male sex when compared to female sex in most parts of the world, which likely reflects complex interactions between sex-specific exposure to risk factors and protective effects of both endogenous and exogenous hormones, as well as gender-specific differences in screening ratios.[2]

However, the incidence and mortality among adults aged 55 years and older have shown a decline for several decades, particularly among adults aged 65 years old and older. This decrease is due to 2 different factors: decrease in the exposure to risk factors, as wells as an increased uptake of screening and improved treatment and removal of precancerous adenomas.[2,4] Nevertheless, in adults younger than 55 years old, there was a 51% increase in the incidence of CRC from 1994 to 2014 and an 11% increase in mortality from 2005 to 2015.[4]

Like mentioned in 1.1., CRC represents 10.2% of all cases of cancer worldwide and 9.2% of the total cancer deaths, being the third most common cancer worldwide and the fourth most common cause of oncological death.[2,3] 55% of all the CRC cases occur in developed or developing countries, which may reflect an increased prevalence of risk factors for CRC associated with the western lifestyle. This risk factors include cigarette smoking, excess body weight, diet (including high consumption of alcohol, as well as red and processed meat and low consumption of fruits, vegetables, dietary fiber and calcium) and physical inactivity.[2,4]

From this data it is possible to conclude that lifestyle modifications are an important tool to reduce the incidence and therefore the mortality rates of this type of cancer. However, the risk of developing CRC is also associated with several hereditary conditions (family history of CRC, medical conditions including chronic inflammatory bowel disease and type 2 diabetes and a history of abdominal or pelvic radiation for a previous cancer.[4] Although most of the CRCs are sporadic, a small percentage arises in the setting of inherited syndromes, such as familial adenomatous polyposis (FAP), juvenile polyposis syndrome (JPS) and Lynch syndrome).[5,6]

An early detection and removal of precursor lesions detected during routine screenings have been shown to significantly reduce incidence and mortality. [4]

1.2.2. Localization and development

It is important to have a better understanding of the mechanisms responsible for tumor initiation and progression in order to develop novel and more powerful therapies against colorectal cancer. Until recently, tumors cells were perceived as being all tumorigenic, however, these line of thought has changed by the identification of cancer stem cells (CSCs).[5] According to this theory, these are the only type of cells capable of initiating a tumor on the primary site or during metastasization.

CRC originates from epithelial cells lining the gastrointestinal tract that undergoes sequential mutations in specific DNA sequences that disrupt normal mechanisms of proliferation and self-renewal.[5]

The intestinal tract consists of the small intestine (duodenum, jejunum and ileum) and the large intestine or colon, which can be sectioned into 4 parts (proximal to distal): cecum; ascending, transverse and descending colon; sigmoid colon; rectum and anal canal. [5] The colon is a tubular organ, with approximately 90 to 150 cm with the main functions of absorption of water, electrolytes and storage of intraluminal contents to allow for controlled elimination of the feces.[7] It presents an interior layer made of absorptive and secretory epithelial, which is folded into invaginations to form the functional unit of the intestine (crypts of Lieberkühn), (figure 2). Each crypt contains about 2000 cells and comprises differentiated cell lineages (enterocytes, enteroendocrine cells, goblet cells and Paneth-like cells).[5]

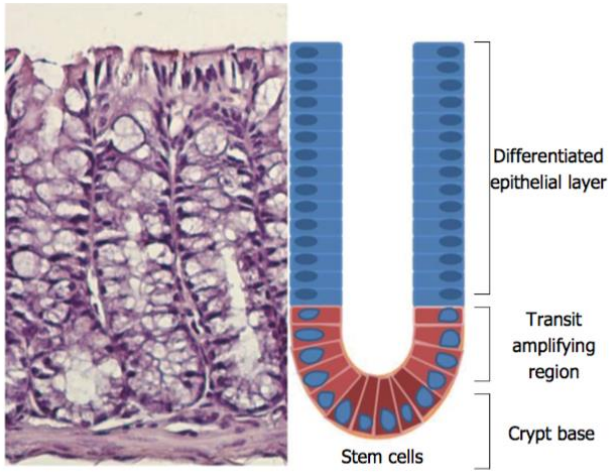

Figure 2 - Representation of a colon crypt. Stem cells lie at the bottom of the crypt and are responsible for generating all epithelial cell types along the crypt (adapted). [5]

Approximately, every 5 days, each colon epithelial cell is replaced, and the number of long-lived stem cells per crypt is estimated to be between 4 and 6 cells.[5] Therefore, stem cells play a key role in regulating the homeostasis of the colonic epithelium.

Regardless of the cause for the beginning of the CRC, the final result is a set of genetic alterations that lead to a normal epithelial cell to become a colon cancer cell. [5] The most widely accepted model for the development of the CRC is the adenoma-cancer sequence,

showed in figure 3. This model describes a stepwise progression from normal to dysplastic epithelium to carcinoma, and according to which, the CRC development occurs through a series of steps: first takes place the localized proliferation of the colon epithelium with formation of small adenomas, which progressively grow with dysplasia and ultimately progress into invasive carcinomas. The adenomas can appear and peak at least 5 years before colorectal cancers. [5,8,9]

Moreover, according to studies performed on patients with FAP during the development process of adenomas, it was shown various degrees of differentiation within human CRC, including a stem cell overpopulation at the bottom of the crypt, thus suggesting a hierarchical model of CRC.[5,10] Although this model can be seen as an oversimplification, it aligns with observed clinicopathological changes with genetic abnormalities in the progression of CRC.[9]

An important mechanism in the CRC formation is the epithelial to mesenchymal transition (EMT) – biological process that allows the polarized epithelial cell, which normally interacts with the basement membrane to undergo multiple biochemical changes that enable it to assume a mesenchymal phenotype which includes enhanced migratory capacity, invasiveness, resistance to apoptosis and increased production of ECM components. [11]

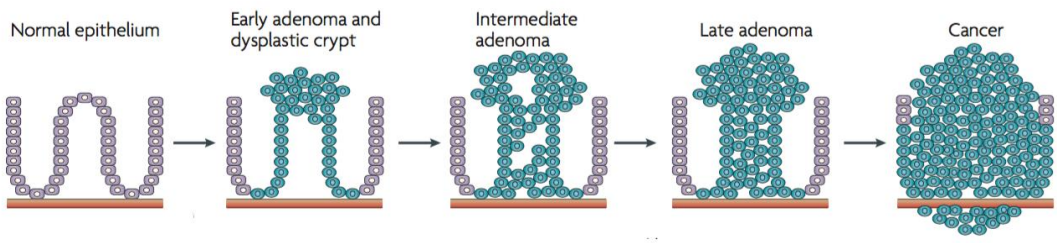

Figure 3 – Adenoma-carcinoma sequence model, by stage, in colorectal cancer (adapted).[9]

An epithelium is a collection of cells forming a relatively thin sheet or layer, being these cells mutually adherent laterally by cell-to-cell junctions. This layer is polarized, with 2 non-identical sides where they can be defined as inside and outside (apical and basal). All the cells show an identical apicobasal polarity, supported on the basal surface by a layer of ECM – the basal lamina. On the other hand, mesenchyme cells form a diffuse tissue network, without a complete cellular layer, and the cells usually only have points on the surface in adhesion to their neighbours.[12]

1.2.3. Cancer Stem cells in CRC

Stem cells are cells that have the ability to differentiate into other types of cells (multilineage differentiation), but also to divide, producing more stem cells of the same type. This ability to multiply is called self-renewal and it is one of the most distinct features of stem cells. [13]

It is known that cancer results from the accumulation of mutations in a single target cell, sometimes over a period of many years. Since stem cells are the only long-lived cells in most

tissues, this suggests that they are the cells in which early mutations leading to cancer accumulate. Additionally, stem cells are the only normal cells that share cancer cells' intrinsic ability to self-renew. Taken together, these facts suggest that, in some cases, stem cells may be the target cells for neoplastic transformation (conversion of a normal tissue with a normal growth pattern into a malignant tumor) – figure 4. Therefore, a tumor can be viewed as an aberrant organ initiated by a tumorigenic cancer cell (stem cell) that acquired the capacity for indefinite proliferation through accumulated mutations that drives the tumor growth. [14]

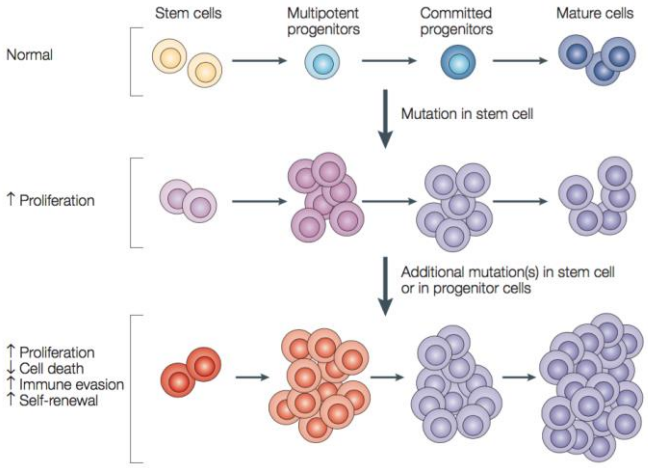

Figure 4 – Model for the development of Cancer Stem Cells: mutations in the stem cell give rise to a stem cell with aberrant proliferation and results in pre-malignant lesion. Additional mutations lead to further increased proliferation, decreased apoptosis, evasion of the immune system and continued expansion of the stem cell compartment, typical of malignant tumors.[15]

Compared to the 'normal' stem cells, the cancer stem cells (CSC) are believed to have no control on the cell number. CSC model relies on four premises: i) a substantial fraction of cellular heterogeneity observed in tumors results from its hierarchical organization, which is often reminiscent of the hierarchy in the tissue of origin; ii) tumor hierarchies are fueled by rare self-renewing CSCs (normally quiescent), whereas the bulk of the tumor is composed of non-CSCs that do not contribute to long term growth; iii) CSC identity is hardwired, meaning that there is limited plasticity in the tumor hierarchy; iv) CSCs are resistant to standard chemotherapy and radiation treatments, which target, preferentially, non-CSCs. Therefore, a cancer stem cell is a cell within a tumor that is responsible for maintaining the growth of the tumor; it is the only cell population within a tumor that has the ability to form a new tumor and can produce progeny of multiple phenotypes. Similarly to normal stem cells, these CSCs would be located in a niche with mesenchymal cells that would ensure their survival in a secure environment, regulating their proliferation through secretion of soluble factors. the discovery of stem cells in the majority of normal tissues, including colon crypts, supports the hypothesis that normal stem cells might represent a possible target for tumorigenic mutations. [5,14,16,17]

The above mentioned premises are the basic pillars of the Cancer Stem Cell Theory schematized on figure 5: this hypothesis is supported by three key experimental observations

initially performed on human acute myeloid leukemia and after extended to human solid tumors: (*i*) only a minority of cancer cells within each tumor is endowed with tumorigenic potential when transplanted into immunodeficient mice, (*ii*) tumorigenic cancer cells are characterized by a distinctive profile of surface markers and can be differentially and reproducibly isolated from nontumorigenic ones by flow cytometry, and (*iii*) tumors grown from tumorigenic cells contain mixed populations of both tumorigenic and nontumorigenic cancer cells, thus recreating the full phenotypic heterogeneity of the parent tumor. [18]

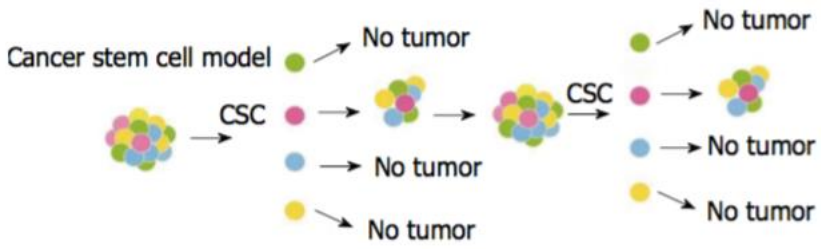

Figure 5 – Cancer Stem Cell model: only a rare subpopulation of undifferentiated cells has the necessary properties for tumor initiation, maintenance and spreading (adapted).[5]

Although there exists a variety of traditional targeting agents for the treatment of patients with CRC, and multiple combination therapies, there is not a curative solution available. This strengthens the model of CSCs and supports the hypothesis that most of the currently available therapies only target the bulk of the tumor mass (mainly constituted by proliferating cells) while sparing the rare, quiescent CSCs which are able to re-initiate tumor growth thus giving origin to both recurrences and metastases.[5]

1.2.4. Metastasization

Metastasis is known as the spread of cancer cells from a primary tumor to a secondary location within the body.[19]

During some steps of embryogenesis and organ development, cells within certain epithelia are able to switch back and forth between epithelial and mesenchymal states, via a process named EMT (epithelial to mesenchymal transition).[11] Indeed, cells within a differentiated epithelium can change their phenotype through activation of an EMT pathway, which enables the conversion of epithelial to mesenchymal cells during adulthood. These types of programs can be activated in association with tissue repair and pathological stresses, for example inflammations and high-grade carcinoma. Therefore, it is currently believed that EMT is a mechanism able to initiate an invasive and metastatic behavior of epithelial cancers.[11] EMT is marked by a complex and coordinated set of molecular changes, leading to cell behavioral changes, it is a concept that can be applied to metastatic behavior of carcinoma cells.[12]

There are 3 types of EMT: type 1 is related with implantation, embryo formation and organ development; type 2 is associated with wound healing, tissue regeneration and organ fibrosis

and type 3 occurs in cells who have already undergone genetic and epigenetic changes, specifically in genes that favor clonal outgrowth and development of localized tumors, affecting oncogenes and tumor suppressor genes. The type of cells undergoing type 3 EMT may invade and metastasize.[11]

The process of tumor spreading through an organism is composed of a series of steps and is schematized in figure 6. Metastases arise from the spreading of cancer from a primary site and subsequent formation of new tumors in distant organs. The metastasization consists of a series of steps, starting with angiogenesis – as the primary tumor grows, it needs to develop a blood supply that can support its metabolic needs. These new blood vessels can also have the function of providing an escape route by which cancer cells can exit the tumor site and enter into the bloodstream (intravasation), tumor cells can also migrate to the blood stream, indirectly, through the lymphatic system. Once these cells arrest in a new organ, they migrate from the circulation into the surrounding tissue: cancer cells deform to fit the vasculature and migrate to new sites, depending on the blood pressure in the new organ. Once in the new site, cells can turn into solitary cells or initiate small pre-angiogenic metastases or larger vascularized metastases. While a small subset of cells executes this action, most of them undergo dormancy or die. These dormant cells are a potential target in premature metastasis detection, concretely in the mesenchymal transition and can be explored as a prognostic maker. On the other hand, solitary cells and micrometastases are clinically undetectable. Only the vascularized metastases are clinically detectable and maintain their growth to form preangiogenic micrometastases; this growth must be sustained by the development of new blood vessels in order for a macroscopic tumor to form. Some types of cancer show an organ specific pattern of metastasization, for example, CRC presents a tendency to metastasize mainly to the liver, however evidence shows that it metastasizes also to the thorax, nervous system, bone and peritoneum. [11,19–21]

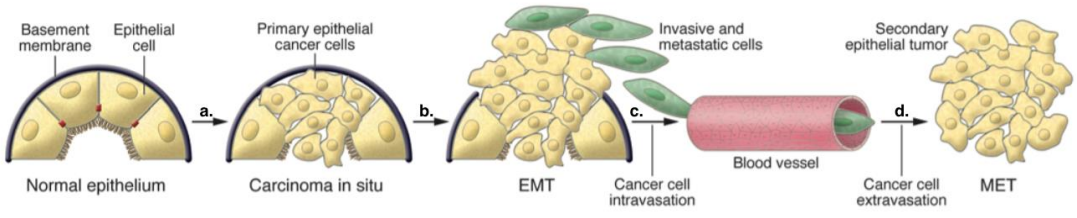

Figure 6 – Steps of progression from normal epithelium to invasive carcinoma: acquisition of genetic/epigenetic alterations – a.; epithelial cells loose polarity and detach from the basement membrane (EMT) – b.; intravasation to the vascular circulation – c.; extravasation and mesenchymal-epithelial transition with angiogenesis giving rise to a secondary tumor – d. (adapted). [11]

Despite the current knowledge on metastasization, the incompetence to treat the said metastasis results in cancer-related deaths, which remains a challenge to modern oncologists until now.[19]

A number of molecules are able to change in expression, distribution and function during the EMT and metastasization and are summarized on table 1.

Table 1 – Classes of molecules that are involved in EMT.[12]

Classification	Molecule
Growth Factor	Transforming Growth Factor : TGF-β
	Wnt
Transcription Factors	Snails
	SMAD
	LEF
	Nuclear β-catenin
Cell-to-cell Adhesion axis	Cadherins
	Catenins
Cell-to-ECM adhesion axis	Integrins Focal contact proteins ECM proteins
Cytoskeletal Modulators	Rho family
Extracellular Proteases	Matrix metalloproteinases Plasminogen activators

The molecules discriminated on the table 1 regulate the metastatic process: for example, changes in cell-to-cell adhesion are promoted by the loss of E-Cadherin; the apicobasal polarity as well as the tissue architecture is changed due to the nuclear β-catenin and activation of transcription factors like Snail and LEF.[12] In its turn, in many late-stage tumors, TGF- β signaling is redirected away from suppressing cell proliferation and is found to activate the EMT, which confers to cancer cells traits associated with high-grade malignancy. [22]

1.2.5. CRC Stem Cells markers

Identifying the CSCs surface markers and intracellular molecules is an important hallmark in the fight against CRC and all types of cancer. In this field, the use of easier antibody techniques such as immunostaining, Fluorescence-Activated Cell Sorting analysis (FACS), cell sorting, etc, allows for the identification and isolation of CSC.[5]

Some of the CRC most important stem cell markers are listed on table 2.

Table 2 – Colorectal cancer Stem Cell markers ant their function.[5,23–26]

Marker	Function
CD133	Transmembrane glycoprotein, which marks tumor-initiating cells within the bulk of CRC, related with self-renewal and tumor angiogenesis.
CD44	Cell adhesion molecule, involved in lymph node homing and lymphocyte activation. Also a hyaluronic acid receptor
Lgr5	Receptor for R-spondin proteins and marker for adult stem cells. Wnt target gene.
ALDH1	Enzymes that are involved in cellular detoxification, differentiation, and drug resistance by oxidation of cellular aldehydes
EpCAM	Epithelial cell adhesion molecule
CD24	Mucin-like cell adhesion molecule.
CD29	Receptor for extracellular matrix proteins involved in regulation of cell migration, proliferation, survival, differentiation and death. Cell adhesion molecule
CD166	Cell adhesion molecule

The CD133+ population is enriched in cancer-initiating cells in many tissues, including colon carcinomas, with studies also indicating a role for *CD133* in tumor angiogenesis. In the intestine, *CD133* would mark stem cells susceptible to neoplastic transformations, which would be prone to aberrantly activate Wnt signaling, disrupting normal tissue maintenance leading to aberrant expression.[23] *CD44* and its variants are associated with the dissemination of isolated tumors and the presence of metastases, it mediates cell-cell and cell-ECM interactions trough binding to its ligand hyaluronan and contributes to tumorigenicity through various mechanisms.[24,25] *ALDH1* is a gene located on chromosome 12, which expresses a type of detoxifying enzyme that contributes to the oxidation of intracellular aldehydes, it confers resistance to alkylating chemotherapeutic agents and protects against oxidative damage by catalyzing the irreversible oxidization of cellular aldehydes. *ALDH1* acts as a promoter, inducing EMT in cancer cells and can be used to identify and isolate normal and cancer stem cells.[27,28] *LGR5* overexpression has been associated with early stages of tumorigenesis, invasiveness and metastization. This is a gene encoding for a component of the Wnt pathway. [29]

1.2.6. Related molecular pathways

Most of the CRC is characterized by a dysfunctional regulation of the Wnt/β-Catenin pathway, essential for the development of the normal mucosa. Normally, this pathway helps determine the cell fate and regulates cell proliferation, it controls the level of key modulator β-Catenin through processes of phosphorylation and ubiquitin-mediated degradation. The Wnt signal is transduced when Wnt proteins bind to the membrane-bound frizzled receptors and coreceptors (LRP 5 and 6). In the absence of Wnt, β-Catenin is bound to a protein complex consisting of axin, adenomatous polyposis coli (APC) proteins, casei-kinase 1α (CK1) and

glycogen synthase kinase 3β (GSK3β). This complex is known as the destruction complex and phosphorylates β-Catenin, allowing it to be targeted for ubiquitinylation and destroyed by the proteasomes. This destruction keeps the levels of β-Catenin low and stops it relocating to the nucleus, where it binds to the T-cell factor/lymphoid enhancer factor (TCF/LEF) proteins. This group can either act as a transcriptional repressor or an activator, depending on the complex they form.[30–32]

Aberrant Wnt signaling is associated with various types of cancer and usually leads to increased levels of β-Catenin in the nucleous. In fact, the malignancy most strongly linked to aberrant Wnt signaling is the CRC. At the bottom of the crypts lie stem cells that produce proliferating precursor epithelial cells. These cells populate the bottom of the crypt and are capable of migrating to the top. This process is controlled by Wnt proteins that are secreted by the stromal cells. Once the precursor cells reach the top, they stop proliferating and after about a week, they undergo apoptosis and are replaced by new cells. In CRC, mutations in the Wnt pathway distort this process and the cells divide uncontrollably and do not undergo programmed death. Most of the mutations in the Wnt signaling pathway occur in the *APC* gene, and this is the earliest genetic alteration in the genesis of CRC, other mutations occur in the *AXIN2* gene and a smaller proportion in the β-Catenin gene (*CTNNB1)* itself. APC is a multifunctional tumor suppressor protein. Loss of some of the function of the APC protein results in constitutive activation of Wnt signaling and in chromosomal instability in human colorectal adenocarcinomas. *AXIN2* is a negative Wnt regulator and tumor suppressor that is found mutated in sporadic CRC and in some familial cancer syndromes. β-Catenin is a key transcription modulator of the Wnt signaling pathway and also a subunit of cadherin protein complexes that plays an essential role in coordinating cell-cell adhesion. Aberrant Wnt signaling is also a crucial factor in the EMT of cancer cells, which, as discussed previously, promotes cancer intravasation and metastasis.[31–33]

The Wnt signaling pathway is involved in most CRC following the principal CRC tumorigenic pathways. However, it plays a major role in the Chromosomal Instability *Pathway* (*CIN* pathway), characterized by widespread loss of heterozygosis and gross chromosomal abnormalities and which encompasses most of the CRC. Alterations in the Wnt signaling pathway are the first step of the CIN pathway, which are then followed by alterations in the *RAS Pathway* thus facilitating tumor progression from benign to malignant stage (the adenoma to carcinoma transition is firstly determined by the *K-ras* gene). In the later stages of the CIN pathway mutations or loss of the *TP53* gene *and the resulting loss of functi*on of the *p53* protein, and subsequent stimulation of the high proliferative activity through the loss of cell cycle control and apoptosis. [34]

The Wnt and the Sonic Hedgehog (SHH) pathways have long been known to direct the growth and patterning during embryonic development. Evidence also implicates these two pathways in regulating stem cell number in epithelia such as those present in skin and intestine.[35] The SHH signaling is a major regulator in cell differentiation, cell proliferation and

tissue polarity. Aberrant activation of the SHH pathway has been shown in a variety of human cancers, tumorigenesis, tumor progression and therapeutic responses have all been shown to impact the SHH pathway.[36]

A large proportion of CRCs display mutational inactivation of the TGF-β pathway, yet, paradoxically, they are characterized by elevated TGF-β production. Mutational inactivation of this signaling pathway is key during CRC progression. Alterations in TGF-β pathway components are first detected in advanced adenomas and affect 40-50% of all CRCs. For example, in mouse models, mutations in the tumor suppressor Apc combined with inactivation of TGF-β signaling components in epithelial intestinal cells trigger the development of invasive adenocarcinomas.[37]

1.2.7. CRC Treatment

Traditionally, there are six hallmarks of cancer that enable tumor growth and metastatic dissemination: sustaining proliferative signaling, evading growth suppressors, activating invasion and metastasis, enabling replicative immortality, inducing angiogenesis and resisting cell death (figure 7). These hallmarks have provided a solid foundation for understanding the biology of cancer.[22]

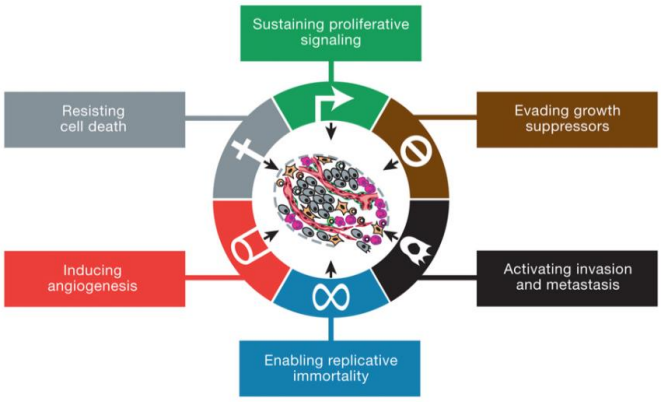

Figure 7 – The six traditional hallmarks of cancer.[22]

However, an increasing body of research suggests that 2 additional hallmarks and 2 enabling characteristics should be noted as they are involved in the pathogenesis of some or all the cancers: deregulating cellular energetics, avoiding immune destruction, genome instability and mutation and tumor promoting inflamation.[22] Therefore, mechanism-based targeted therapies to treat human cancer are one of the fruits of 30 years of progress of research into the mechanisms of cancer pathogenesis. The set of targeted therapeutics can be categorized according to their effect on one or more hallmarks already described (figure 8).[22]

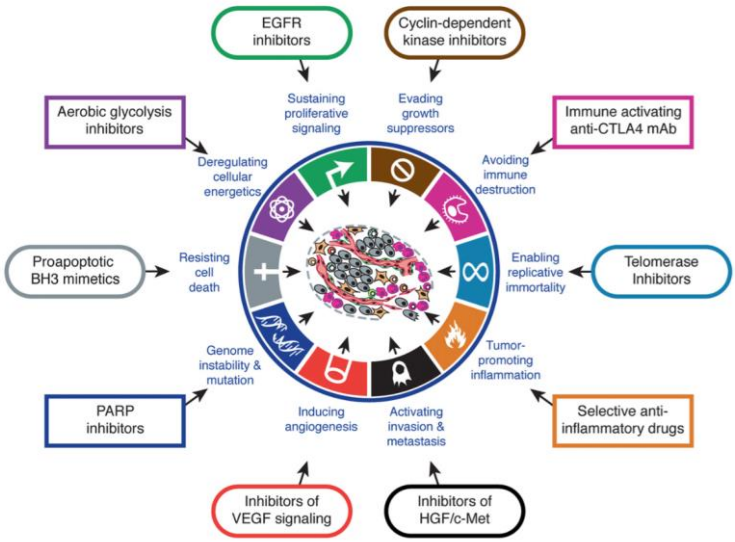

Figure 8 – Therapeutic targeting and its relationship to the hallmarks of cancer. Representation of the drugs that interfere with each of the characteristics necessary for tumor growth and progression.[22]

For most localized tumors, surgery, radiotherapy and chemotherapy are the primary treatments, and although it may be curative for some patients, the presence of micrometastases will lead to the relapse and death of a substantial proportion.[38] Currently, some of the most used chemotherapeutical agents are 5-Fluorouracil (a fluorinated pyrimidine), oxaliplatin and irinocetan. [39–41]

Cancer cells can acquire resistance to chemotherapy by a range of mechanisms, including mutations or overexpression of the drug target, inactivation of the drug or elimination of the drug from the cell. Apoptosis occurs to maintain the homeostasis replacement of cells in tissues, mediated by a class of cysteine proteases called caspases. Failure to eliminate cells may also contribute to the development of cancer and cancer resistance to anticancer therapy, therefore, the enhancement of cell apoptosis is one possible approach to cancer control by anticancer agents.[42,43]

Cancer is not a bulk of cancer cells, its formation resembles an organogenesis with its beginning in a population of cancer stem cells. The failure to eradicate this population of cells may result in the reoccurrence and metastasization of cancer, (figure 9).

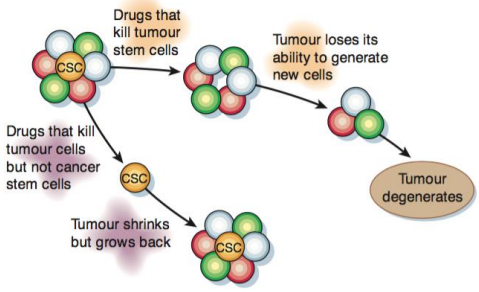

Figure 9 - Conventional treatment of cancer vs. treatment targeting cancer stem cells. If therapies can be targeted against cancer stem cells, they might be more effective in degenerating the tumor or preventing it to grow.[44]

This new dimension of tumor heterogeneity interferes with conventional cancer treatments such as chemotherapy and radiotherapy: CSCs present a higher resistance to these types of therapies. This resistance helps to explain the often disease reoccurrence following apparently successful treatment of human solid tumors. Therefore, CSCs may represent a double-threat once they are more resistant to the said conventional therapies as well as being able to regenerate a tumor once the therapy is concluded. [22] Moreover, CSCs are highly resistant to traditional antineoplastic agents due to the expression of detoxifying enzymes, drug transporters and DNA repair mechanisms. The CSC theory supports the need of a better characterization of CSCs with the goal of developing CSC-specific therapies, which may represent a great advantage in the fight against cancer. [30] The development of biologically targeted drugs will potentially allow for a higher efficacy rate and less unwanted effects on cancer treatment. [38]

1.3. Colorectal cancer cell models

Cancer research is highly dependent on representative and reliable model systems, it is heterogenic and a rather complex set of individual diseases, which makes research on cancer very difficult, expensive and requires enormous resources. The models used have changed constantly and evolved to all the stages of drug discovery and nowadays, the selection of the best model to mimic the tumor entity is one of the major challenges for cancer researchers.[45]

1.3.1. 3D cell models

The amount of cancer therapeutics that successfully transition into clinical trials is low, due to several factors including the sub-optimal pre-clinical validation, complicated nature of the disease itself and limited clinical assay tools. Until recent years, *in vitro* screenings of synthetic and natural products for the development of new drugs relied on assays using established cell lines grown as 2D cultures, which have a rapid, uncontrolled growth phenotype. These types of assays present several advantages, and have contributed greatly to the knowledge on cancer biology. However, they represent several limitations such as: they are not able to mimic the complexity and heterogeneity of clinical tumors as these grow in a 3D conformation with specific organization and architecture. Therefore, a number of signals and mechanisms that regulate cellular processes are lost when cells are grown in a monolayer (2D).[19,42,46,47]

3D cell models grown from established immortalized cell lines or primary cell cultures are a more representative model on which to perform *in vitro* drug screenings: they possess several features of *in vivo* tumors such as cell-cell and cell-ECM interactions, hypoxia, oxygen, nutrient and waste gradients, drug penetration, response and resistance, production and deposition of ECM. An ideal 3D culture model simulates a tissue specific physiological or pathophysiological disease microenvironment, where cells proliferate, aggregate and differentiate.[19,46,48]

There are two main types of 3D models: scaffold-based models and non-scaffold, anchorage-independent models. A scaffold is a temporary structure that supports cells in a given environment and can eventually be incorporated into the tissue. Scaffold platforms are usually made of synthetic or naturally derived polymers that provide support for the growth of the cells and mimicking the ECM conditions. These type of models usually better mimics the cell-ECM interactions. On the other hand, tumor spheroids are one of the most versatile and common scaffold-free model for 3D cell culture, which can be self-assembled or forced to grow as cell clusters starting from single suspensions; these are spherically symmetric aggregates of cells with no artificial substrate for cell attachment. The spheroids are a better representation for study of the physiological gradients and serve as a tool to investigate the regulators of tumor microenvironment or responsiveness to therapeutics associated with metabolic and proliferative gradients such as altered sensitivity of hypoxic tumor cells or chemotherapeutic resistance. Some of the traditional 3D cell culture models are spinner flasks and gyratory rotation devices. [19,42,46–48]

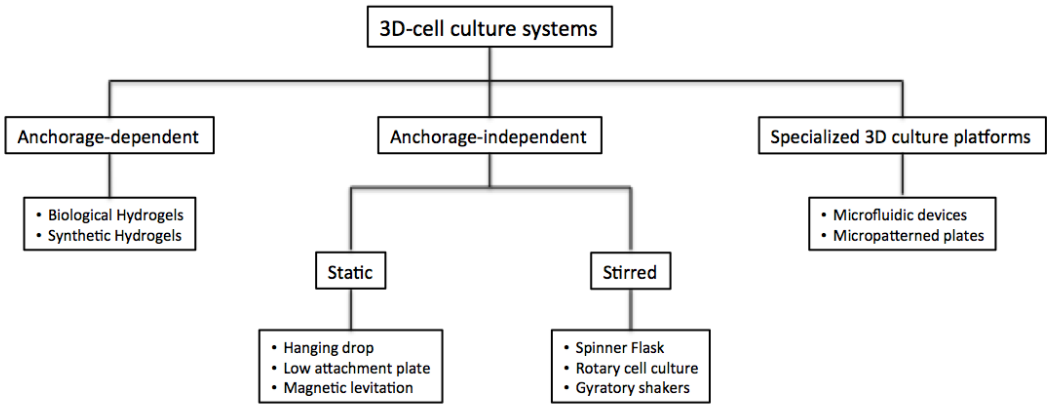

Figure 10 – Different types of three-dimensional cell culture systems.[42,48]

As schematized in figure 10, there are multiple 3D cell model culture strategies. Anchorage dependent technologies provide physical support ranging from simple mechanical structures to ECM-like matrices where cells can aggregate, proliferate and migrate. However these types of cultures are not representative of the *in vivo* environment, besides, the chemical and physical properties of the scaffold can influence the cells behavior. Another 3D cell culture systems are the anchorage-independent technologies, these rely on self-aggregation of cells either in static conditions or under stirred conditions. Static formation of aggregates takes place either in specialized culture plates such as hanging drop microplates, or in low adhesion plates with ultra-low attachment coating that promotes spheroid formation. For long-term cultivation, non-stagnant culture systems such as the spinner flask are suitable: inside this, cells lack a substrate and as a result they interact with each other and form aggregates. The spinner type of culture already exists for over 30 years but is still one of the most efficient scaffold-free technique in order to obtain a large amount of spheroids under a well controlled

nutrient supply. Other methods such as gyratory shakers or the rotary cell culture are also commonly used. Lastly, the 3D specialized platforms: this type of culture system relies on micropatterned plates that can be designed to enhance cell-to-cell adhesion for scaffold-free microsphere formation within the confinement of a microspace.[42,48]

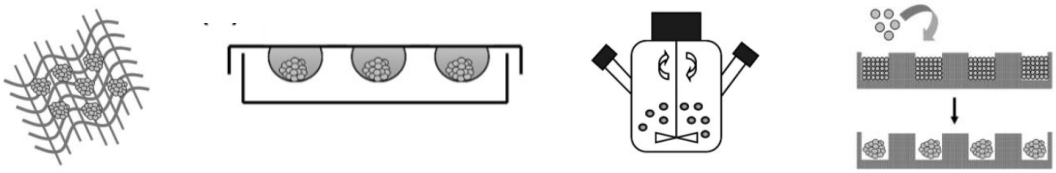

Figure 11 – Examples of 3D culture systems: (A) Anchorage-dependent scaffold; (B) Anchorage-independent static system hanging drop; (C) Anchorage-independent stirred system spinner flask and (D) Specialized 3D culture platform – micropatterned plate. (adapted) [49]

1.3.2. Anchorage Independent 3D cell model

Spheroids consist of actively proliferating cells that aggregate to each other to form a spherical mass: the outside of the spheroid consists of proliferating cells, on the next inner layer, quiescent cells and on the core of the spheroids, dead cells (figure 12). This distribution of cells is due to crescent nutrient deprivation and limitation of O_2 further into the spheroid. Therefore, the microenvironment and architecture of the tumor are better mimicked using these models recapitulating the structure of the living tissue and allowing for a better investigation of the pathobiology of the human cancers.[46,47]

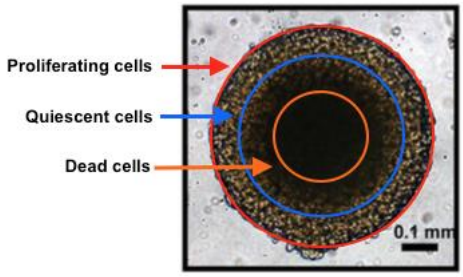

Figure 12 – Example of a 3D spheroid and identification of the different regions of cells within the spheroid (adapted).[47]

The biggest applications of these models is in testing chemotherapeutic agents, new drugs, delivery systems and mapping responses to treatments.[46]

The HT29 cell line is an immortal cell line, which derives from a 44-year-old female Caucasian human, from a colorectal adenocarcinoma.

During past years, the host laboratory (Food Functionality and Bioactives of iBET – Oeiras, Portugal) in collaboration with the Animal Cell Unit of iBET (Oeiras) developed a 3D model of cell aggregates with the HT29 cell line. This model has been used as a pre-clinical model for the testing of natural compounds with chemotherapeutical potential.[50–55]

This model is produced by culturing HT29 cell line under stirred conditions using spinner vessels forming a spherical aggregate. These aggregates grow in 3 stages: aggregation, compaction and growth. During the aggregation phase (first 24 hours), the cellular density is maintained with the formation of clusters of single cells and variable in size; from days 2 to 3 of culture the spheroid diameter remains but the cellular concentration increases, also decreasing the cellular density, which suggests a spheroid fusion (compaction phase). From days 3 until the 7th the spheroids gain the structure described in figure 12 and there is only an increase of size during this growth phase. These different stages are schematized on figure 13 in terms of spheroid diameter and cellular concentration.

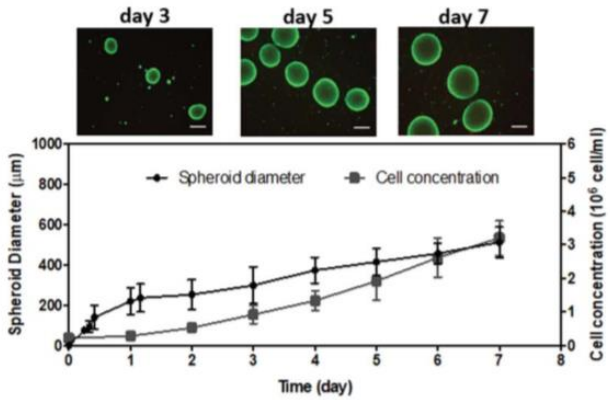

Figure 13 – Aggregation and spheroid growth process on stirred culture system as well as spheroid diameter distribution along culture time. [53]

The spheroids collected after day 7 of culture present characteristics of *in vivo* solid tumors, namely the existence of a necrotic/apoptotic core, hypoxia regions, presence of cancer stem cells and a less differentiated invasive front.[53]

1.4. Virgin olive oil and its anticancer properties

The traditional Mediterranean diet is representative of a healthy lifestyle, being identified as a balanced diet with great potential to prevent diseases associated with oxidative damage, such as cardiovascular diseases and cancer, including colorectal cancer. This is supported with the fact that cancers like CRC present a lower incidence, a lower death rate and a higher life expectancy in Mediterranean countries when compared to Northern Europe. It is estimated that the incidence of cancer could be reduced by 25% if the populations of the Western countries consumed a traditional Mediterranean diet. [56–60]

The components of the traditional Mediterranean diet are: high monounsaturated to saturated fat ratio, moderate alcohol consumption, high consumption of vegetables, cereals and fruits, low consumption of meat and meat products and a moderate consumption of milk and dairy products. Olive oil, a key component of this type of diet, explains the high ratio of monounsaturated to saturated fat and is believed to affect numerous biological processes.[56,57]

Virgin olive oil is the oil obtained from the fruit of the olive tree only by mechanical or physical means (for example cold-press), under conditions that do not alter the oil or its properties.

This oil does not undergo any treatment other than washing, decantation, centrifugation and filtration and it contains a low percentage of free fatty-acids (<1%) and high phenol levels. [57,59] Olive oil contains a vast range of substances such as monounsaturated free fatty acids, hydrocarbon, squalene, tocopherols, and phenolic compounds. Olive oil is a source of at least 30 phenolic compounds and its concentrations and proportions depend on factors like the cultivars, the soil, climate, manner in which the oil is produced and stored and the degree of drupe maturation. Phenolic compounds are more abundant in olive oil than seed oils and can be divided into different classes: simple phenols, secoiridoids, lignans, flavonoids, polyphenols and phenolic acids, all of which have potent antioxidant and anticancer properties. These types of compounds are believed to function as defense mechanism of plant cells against injury during oxidation processes. Phenols are the most studied components in virgin olive oil, with recognized antitumor properties, inhibiting carcinogenesis at the initiation, promotion and progression stages, directly or indirectly linked to antioxidant activity. [56,57,59,61]

The colon, being a major body site involved in the metabolism of phytochemicals, has direct contact with both metabolites and original dietary phenolics. Given the fact that the olive oil phenolics are fat soluble, they are likely absorbed and should have chemopreventive action effect against breast cancer and heart diseases. The phenols present in food can reach the colon by different paths: unabsorbed food fraction, enterohepatic recirculation or deconjugation of metabolites. The phenolics that reach the large intestine will suffer catabolic transformations by microbial metabolism, producing biological metabolites and have chemopreventive effect against colorectal cancer (these have the ability to affect or perturb crucial factors that control cell proliferation). When compared to other organs, the concentration of phenolics and its metabolites on the gastrointestinal tract is higher, where they are believed to be able to both direct reaction with reactive oxygen species (ROS) and prevent their formation.[43,56,57]

Oxidative stress is due to an imbalance between the oxidant and antioxidant systems of the organism, in favor of the oxidant. Oxidation is mainly caused by free radicals and the related ROS, these free radicals are able to damage fatty acids and to provoke a chain reaction called lipid peroxidation, which may lead to loss of membrane function and integrity, and in the end, apoptosis and necrosis.[59]

The gastrointestinal tract is colonized by gut microbiota, composed of eukaryotic fungi, *Achaea*, viruses, and bacterial communities, all of whom contribute for the maintenance of the healthy state of the colon. However, the gastrointestinal tract is constantly exposed to harmful substances, like pathogenic microbiota, many of which introduced by diet (including free radicals and lipid oxidation products). Any alterations in the intestinal homeostasis can lead to the formation of ROS, which in turn can provoke structural and functional alterations in the tract tissues. Besides the antioxidant effects of the phenols, they have the potential to

regulate signaling pathways and gene expression involved in cell proliferation, cell cycle control, apoptosis, detoxification enzyme systems and the immune system. [56,57,61]

The most important and abundant complex phenols present in virgin olive oil are tyrosol, hydroxytyrosol and oleuropein (whose molecular structure is represented in figure 14). These 3 compounds have a similar structure and there is evidence that they could reduce oxidative damage to cellular DNA and reduce the amount of potentially carcinogenic products of lipid peroxidation upon olive oil storage, decreasing the development of CRC. [59]

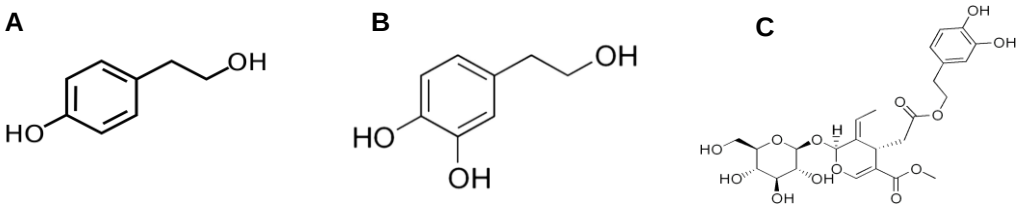

Figure 14 – (A) tyrosol, (B) hydroxytyrosol and (C) oleuropein molecular structures.

1.4.1. Hydroxytyrosol

Hydroxytyrosol (HT) is the most important phenolic compound in virgin olive oil. This bioactive compound can be found in higher concentration in virgin olive oil (14.42 ± 3.01 mg/kg). It is a potent antioxidant and has several biological activities: significant anti-inflammatory, control of oxidative stress, inhibition of several tumor cell lines as a chemotherapeutic agent, and apoptosis promoter, improving endothelial cell function, having protective effect on liver steatosis and presenting neuroprotective effects as well. This compound may exert antitumor activity on human colon adenocarcinoma cells, affecting the transcription of genes involved in programmed cell death and activating Caspase-3. HT also enhances carcinogen detoxification and upregulates xenobiotic metabolizing enzymes.[43,59,62]

During gastric digestion, complex virgin olive oil phenols (oleuropein, derivatives or secoiroids) are transformed into HT, which is later transformed into metabolites and HT-acetate by the acetyl-CoA activity. Once the unmetabolized native phenols arrive at the small and large intestines, the microbiota transforms them into different catabolites by oxidation and dehydroxilation reactions: HT is thoroughly transformed into phenylacetic acid and its derivatives and the catabolism of HT-acetate produces phenylpropionic derivatives, allowing for the absorption of these colonic metabolites.[43] In figure 15 are shown 2 of the HT metabolites, phenylacetic acid and phenylpropionic acid.

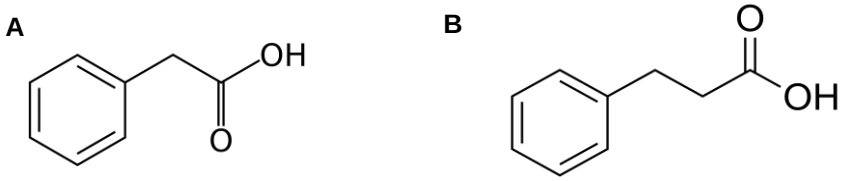

Figure 15 – (A) Phenylacetic acid molecule structure; (B) Phenylpropionic acid molecule structure

Previous studies showed that a moderate daily consumption of olive oil rich in its own phenols raised the concentration of phenylacetic and phenylpropionic acids in human feces, revealing an increase of free hydroxytyrosol. The antiproliferative effect of HT and its main metabolites have been described in CRC cell lines and the results are summarized on table 3.[43,63]

Table 3 – Previous studies performed with HT, PA and PPA on colorectal cancer cell lines and their outcomes.

Cell line	Compounds tested	Outcome	Effective Concentrations	Reference
HT29 and Caco-2	HT, PA and PPA(1)	Cell cycle arrest	ND(2)	[43]
		Promotion of apoptosis	ND(2)	
HT29	HT	Antiproliferative activity	EC_{50} = 60 µM	[62]
		Lack of apoptotic activity	-	
HT29, Caco-2 and WiDr	HT	Antiproliferative activity	EC_{50} (HT29) = 181.8 µM EC_{50} (Caco-2) = 281.64 µM EC_{50} (WiDr) = 278.5 µM	[64]
HT29	HT	Antiproliferative activity	EC_{50} = 750 µM	[65]

(1) HT – hydroxytyrosol; PA – phenylacetic acid; PPA - phenylpropionic acid;

(2) ND – Not Described

Although there are several studies already pointing to the antiproliferative effect of HT, not a lot is known about how it affects the population of cancer stem cells.

1.5. Aim of the thesis

The present study was performed during a timeframe of six months in the research group of Food Functionality and Bioactives (Food and Health Division) in iBET (Oeiras, Portugal), within the scope of an iBETXplore project VOOMICS.

Although there are many studies performed on the effect of hydroxytyrosol and other phenols from olive oil on colorectal cancer, there is few information regarding their effect on Colorectal Cancer Stem Cells. Therefore, this study was performed in order to assess the action of hydroxytyrosol and its colonic metabolites in modulating cancer stemness. For that, a 3D cellular model of CRC already established in the host lab was used .

In a first approach the antiproliferative effect of hydroxytyrosol and two of its colonic metabolites (phenylacetic acid – PA – and phenylpropionic acid – PPA) was evaluated on monolayer cultures of HT29 cell line. During this stage, cytotoxicity assays were also performed using Caco-2 cell line for the screening of the gastrointestinal safety of the same compounds. Then HT29 spheroids that better mimic tumors, containing a high percentage of

CSC, were used to evaluate the effect of olive oil compounds in inhibiting cancer cell proliferation and target stemness using several methodologies: Aldefluor assay, Colony Forming Unit (CFU) assay and Gene expression analysis.

Combination studies were also performed with 5-fluororacil, in order to assess whether the olive oil compounds improve the efficacy of this chemotherapeutic drug. The overview of this thesis plan is show in figure 16.

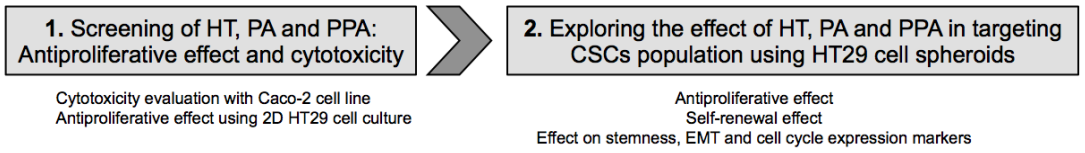

Figure 16 – Work plan for the present study organized in two main tasks

2. Experimental Procedure

2.1. Cell culture and cell lines

For this study, three cell lines were used: HT29 obtained from American Type Culture Collection (ATCC, Manassas, VA, USA) and Caco-2 purchased from Deutsche Sammlung von Microorganismen und Zellkulturen (Barunshweig, Germany)

HT29 cell line derives from a 44-year-old female Caucasian human, presents an epithelial morphology and these cells are from a colorectal adenocarcinoma. This cell line was used between the passages 28 and 51. Caco-2 cell line is from a 72-year-old Caucasian human male, from a colorectal adenocarcinoma and their morphology, like HT29, is epithelial-like. Caco-2 cells were used between passages 28 and 50.

All the cell lines were cultured in RPMI 1640 medium supplemented with 10% (v/v) heat-inactivated fetal bovine serum (FBS). Caco-2 was additionally supplemented with 1% (v/v) penicillin-streptomycin. All the culture medium and supplements were obtained from GIBCO® (Thermo Fisher Scientific, MA, USA).

The cell lines were kept in a humidified atmosphere at 37ºC and 5% CO_2 using an incubator NuAireTM US Autoflow,UK (monitored daily) and subcultured once or twice or three times a week, when obtained a confluency between 80%-90% and according to the need for the assays, in 75 or 175 cm^2 T-flasks. For the detachment of the cells from the T-flasks, trypsin/EDTA (purchased from Gibco, Thermo Fisher Scientific, MA, USA) was used.

2.2. Cell counting using trypan blue dye

For most of the assays performed, it was necessary to count the number of viable cells. In order to do so, it was performed the trypan blue exclusion method, using the hemocytometer and trypan blue dye. Cells were diluted at the desired ratio in 0,1% (v/v) of trypan blue solution in MiliQ water (and PBS when necessary), in order to obtain a minimum of 20 cells per square and a maximum of 50. 20 μL of this solution was placed in each side of a Fuchs-Rosenthal hemocytometer counter and the viable and dead cells were counted on the inverted microscope (model CKX41 from Olympus®). Equation 1 was used to determine the concentration of cells.

$$Cell\ concentration\ \left(\frac{cell}{ml}\right) = \frac{Cells\ in\ square\ 1 + Cells\ in\ square\ 2}{Number\ of\ counted\ squares} \times dilution\ factor \times 5000 \qquad (1)$$

Dead cells could be distinguished from live ones by the difference in colors. Viable cells maintain the plasmatic membrane intact and therefore, the dye cannot penetrate to the interior of the cell. However, dead cells' plasmatic membrane gets disrupted and allows for

the entrance of the dye. Therefore, dead cells present a dark blue color, being clearly distinguishable from the live ones who present a more clear and bright aspect.

2.3. VOO compounds and metabolites

Hydroxytyrosol was purchased from Extrasythese® (Genay, France) with a purity of >99%. Phenylacetic acid and phenylpropionic acid were purchased from Sigma-Aldrich® (Sigma-Aldrich, St. Louis, MO, USA) and presented a purity of 99% and 97% respectively. 5-fluororacil (5-FU) was also obtained from Sigma-Aldrich® (Sigma-Aldrich, St. Louis, MO, USA). The stock solutions of hydroxytyrosol, phenylacetic acid and phenylpropionic acid were prepared in miliQ water at a concentration of 20mM and stored at - 20ºC. 5-FU stock solution was prepared with miliQ water for a final concentration of 5mg/mL and also stored at - 20ºC.

All the stock solutions were filtered prior to the use in cell assays.

For the cell-based assays, the necessary amount of the stock solutions were diluted in RPMI medium supplemented with 0.5% (v/v) FBS. All the stock solutions were filtered prior to the use in cell assays. In all the experiments, it was included a control only with cell medium and another control where the cells were incubated with culture medium and water for a final concentration of up to 25% (v/v).

2.4. Cytotoxicity assay using Caco-2 cell line

This assay was performed as described by Serra et al. [66] and intended to evaluate, *in vitro*, the cytotoxicity of HT and its colonic metabolites PA and PPA, using Caco-2 cell line. This cell line, as referred in 2.1., is from a human colon adenocarcinoma. However, when cultured under special conditions, it leads to a monolayer growth of cells with several morphological and functional characteristics resembling mature enterocytes.[67] This characteristics are obtained after 7 days of seeding and after the monolayer attains approximately 80% to 90% of confluency.

Briefly, cells were seeded on 96-well plates at a density of 2×10^4 cells/well and the medium was replaced every 48h (RPMI + 10% (v/v) FBS + 1% (v/v) PEN). After confluency (more or less 7 days), Caco-2 cells were incubated with the compounds diluted in low-serum culture medium (RPMI + 0.5% (v/v) FBS) for 72h. The concentration of the compounds ranged between 125 µM and 2000 µM. Two control samples were also prepared, one with low-serum culture medium and the other with the maximum % (v/v) of the solvent (in the present work this control was prepared with water). The goal of this control with the solvent is to insure that the effects observed are caused by the compounds and not by the solvent (dilution effect of the culture medium). After this period of 72h, the cells were washed twice with 100 μL of warm PBS per well, and 100 µL of colorimetric reagent MTT was added to each well with a concentration of 0.5 mg/ml with RPMI 0.5% (v/v) FBS and incubated at 37ºC and 5% CO_2 for

3 hours. MTT is reduced to a purple formazan product by mitochondrial reductase enzymes, active in viable cells. Therefore the amount of formazan is proportional to the number of viable cells. After 3 hours of incubation, the cell medium was removed and DMSO was added to each well (150 μL/well). Formazan was quantified by measuring the absorbance of each well at 570nm in a microplate reader Epoch 2 from Bioteck Instruments, (Winooski, VT, USA). 5 independent experiments were performed with triplicates for each condition and the results are shown as percentage of living cells relative to the control. GraphPad Prism 6 (GraphPad Software, Inc., CA) was used for plot the data, as well as for the calculation of the inhibitory concentration required to reduce 50% of cell viability (EC_{50} value).

2.5. Antiproliferative assay using HT29 cell line cultured in monolayer (2D cell model)

The potential of HT, PA and PPA to inhibit colorectal cancer cell growth was evaluated in HT29 cells, as described previously.[50,66] Briefly, HT29 cells were inoculated in 96-well plates with a density of 1×10^4 cells/well. After 24h of incubation at 37ºC and 5%CO_2, the medium of each well was replaced by the compounds diluted in RPMI + 0.5% (v/v) FBS. The concentration of the tested compounds ranged between 25 µM and 400 µM. Like described in section 2.4 a medium control and a control with solvent were also used in this assay. After 72h of incubation, the cell viability was assayed by MTT method, as described in section 2.4. Results are shown as percentage of living cells relative to the control and are a mean of triplicates from three independent experiments GraphPad Prism 6 (GraphPad Software, Inc.., CA) was used for plot the data, as well as for the calculation of the inhibitory concentration required to inhibit 50% of cell viability (EC_{50} value).

2.6. 3D cell culture

For the 3D cell culture, a stirred culture system of a 125 mL spinner flasks (Corning, NY, USA) was used.[53] These spinner flasks were silanized prior to use with dimethyldichlorosilane (Merck, Germany) insuring a hydrophobic surface to the walls of the spinner, preventing the attachment of the cells to the walls. Briefly, HT29 cells were grown in a 175 cm^2 until confluency was attained. After a trypsinization step in order to detach the cells from the t-flask surface, the cells were counted as described in 2.2. Afterwards, the cells were inoculated in a 125 mL spinner flask with 60 mL of the standard medium for this type of cells (RPMI +10% (v/v) FBS). The volume of cells inoculated was calculated in order to have a total of 1 million cells on the spinner. Five minutes after inoculation, a new cell counting was performed to verify the cell density inoculated. The spinner was placed on a magnetic stirrer at 40 rpm, 5%CO_2 and 37ºC for 6 hours. After that, 40 mL of cell culture medium was added (RPMI +10% (v/v) FBS), for a total volume of 100 mL, and the agitation speed was increased to 50 rpm at 8h after inoculation and to 60 rpm at 28h after inoculation. From the 4th day of culture onwards, half of the culture medium was replaced for fresh medium (RPMI +10% (v/v) FBS)

on a daily basis. Besides replacing the medium, the number of cells/mL of culture was monitored everyday, as well as the spheroids morphology and size using an Olympus® CKX41 inverted microscope. The experiments were performed using spheroids collected at days 7 and 8 of culture.[50,53,55]

2.7. Antiproliferative assay using HT29 spheroids (3D cell model)

The antiproliferative effect of the colonic metabolites of virgin olive oil HT, PA and PPA and the chemotherapeutic 5-fluororacil (well-characterized drug that inhibits cell proliferation) was assessed using spheroids collected at day 8 of culture, as described previously. [50,52–54,68] Briefly, spheroids were seeded at a density of 5 spheroids/well on 96-well plates with 100 μL of cell culture medium (RPMI +10% (v/v) FBS). At time-point 0h, prior to treatment with the compounds, the viability of the cells was evaluated using PrestoBlue Cell Viability Reagent (Life Technologies, Carlsbad, USA). This procedure was done according to the manufacturer's instructions: 10 μL of PrestoBlue was added to each well and after 2 hours of incubation in humidified atmosphere at 5%CO_2 and 37ºC, the plates were centrifuged (200g, 5 min.). The supernatant was then removed to a black 96 well plate and its fluorescence intensity measured on a Microplate Fluorimeter FLx800 (Bioteck Instruments, Winooski, VT, USA) with excitation and emission wavelengths of 560 and 590 nm respectively.

The spheroids were incubated with the compounds with concentrations ranging from 125 μM to 4000 μM and with 5-FU with concentrations ranging from 0.01 mg/mL to 0.32 mg/mL for 72h in humidified atmosphere at 5%CO_2 and 37ºC. Controls were performed with spheroids grown in culture medium RPMI +0.5% (v/v) FBS and in culture medium with the highest percentage (v/v) of solvent used (miliQ water).

After the 72h period of incubation, the plates were centrifuged (200g, 5min.) and the supernatant removed, the spheroids were washed with PBS twice and the step of centrifugation repeated. After the removal of the PBS, cell viability was measured using MTT viability assay, as described in section 2.4., with the modification of a 4 hour incubation period with the reagent. This assay allows for the comparison of the viability at time-point 0h and 72h.

The results were expressed in % of cell viability in relation to the control cells using the following equation:

$$Cell\ viability\ (\%) = \frac{Abs\ (\ treated\ spheroids)_{72h} \Big/ FI\ (treated\ spheroids)_{0h}}{Abs\ (control\ )_{72h} \Big/ FI\ ratio\ (control\ cells)_{0h}} \times 100 \qquad (2)$$

Where FI is the fluorescence intensity obtained at time-point 0h and Abs is the absorbance of the spheroids at 72h.

EC_{50} values were obtained trough dose-response curves using GraphPad Prism 6 (GraphPad Software, Inc., Ca). The assay was performed with 6 replicates of each sample concentration in, at least, 2 independent studies.

2.8. Aldefluor Assay (ALDH) by Fluorescence-activated cell sorting (FACS)

The aim of this assay is to study the effect of the tested compounds on the population of CSCs, through the isolation of cells with high dehydrogenase (ALDH) enzymatic activity. This is a fluorescence-based method that is able to detect the enzymatic activity of the ALDH1 isoform. The mechanism of action is based on the passive diffusion of BODIPY-aminoacetaldehyde (BAAA) (ALDH reagent) into viable cells where it serves as a substract for ALDH1. Therefore, in the presence of ALDH, BAAA is converted into BODIPY-aminoacetate (BAA), which is retained inside the cells. The amount of fluorescence is proportional to the ALDH activity in the cells and was measured using a flow cytometer. The active efflux of the reaction product is inhibited by the inhibitor of the kit (DEAB).[69]

The ALDH assay was performed according with the methodology described elsewhere.[50,54] Briefly, spheroids collected at day 8 of culture were placed, at a density of 50 spheroids /well in a 6-well plate. Spheroids were inoculated with several concentrations of the compounds (HT – 200, 400, 600 µM; PA – 600 and 1400 µM; PPA – 600 and 1400 µM; 5-FU - 0.01mg/ml) previously diluted in RPMI + 0.5% (v/v) FBS). Controls were also performed with spheroids incubated with culture medium and culture medium and solvent (this was prepared using water as solvent). After 72 hours of incubation, the spheroids were collected to eppendorfs and centrifuged 5 min at 200g. Then the supernatant was removed and the spheroids were washed with PBS and centrifuged again in the same conditions mentioned above. After removal of the PBS, the spheroids were dissociated with trypsin (200 µL) and the enzyme activity stopped with complete medium (800 µL). The total cell number was calculated as well as the volume equivalent to 0.5 x 10^6 cells, based on the cell counting using trypan blue assay (section 2.2). Finally, the eppendorfs were centrifuged again and the pellet was resuspended in ALDH buffer. After that, 2.5 µL of ALDH reagent was added to each cell suspension and 250 µL of it were transferred to an eppendorf containing 2.5 µL of the inhibitor DEAB (negative control). Following a 30-45 minute period of incubation in a humidified atmosphere at 5% CO_2 and 37ºC, all the samples were centrifuged again for 5 min at 200g, the supernatant removed, and the pellet resuspended in 250 µL ALDH buffer. Finally, all the samples were kept on ice until being analyzed by the flow cytometer CyFlow® Space (Partec, Germany) and the data measured by the FloMax 3.0 software (Partec, Germany). The collected data was further analyzed with Flowing 2.5 software (Turko Centre for Biotechnology, Finland).

2.9. Soft Agar colony forming unit (CFU) assay

Another type of assay able to analyze the stemness potential of the cells under the effect of the studied compounds is the Soft Agar colony forming unit assay (CFU assay). In this assay, the self renewal ability of cells was evaluated by quantifying if one single cell can give rise to a colony of cells in a semi-solid support. For this, single cells were obtained from dissociation of the spheroids collected at day 7 of culture, as described previously. [50,52,54]

Briefly, the bottom layer of the semi-solid support was obtained from mixing in a 1:1 ratio 1.2% of low-melting agarose (Lonza, Rockland ME, USA) with 2x RPMI with 20% (v/v) FBS resulting in a 0.6% agarose with complete medium solution. 2 mL of this solution was pipetted into each well of a 6-well plate carefully to avoid the formation of bubbles. The plates were left at room temperature inside the laminar flow chamber for 30 min to 1 hour. Regarding the upper layer, 0.6% low-melting agarose (Lonza, Rockland ME, USA) was mixed in a 1:1 ratio with warm PBS to a final volume of 6 ml/falcon (duplicates of 2 wells for each concentration) forming a solution of 0.3% agarose with PBS.

HT29 spheroids collected at day 7 of culture were centrifuged for 200g, during 5 minutes and further submitted to a dissociation protocol with trypsin as described in section 2.8.. Briefly, they were trypsinized into single cells, the number of live and dead cells was counted (as described in section 2.2) and the cell concentration was then calculated. The cells' sample was centrifuged again at 200g for 5 minutes and resuspended in the same volume of PBS to maintain the previously determined cell concentration. The volume of cellular inoculum for a final concentration of cells of 1×10^3 cells/ml was estimated. The inoculum was added to the solution of 0.3% agarose and PBS as well as the compounds to be tested: HT – 5, 10, 20 and 50 µM; PA – 20, 200 and 500 µM; PPA - 20, 200 and 500 µM and 5-FU – 0.001, 0.0001 and 0.00001 mg/ml. Controls were also performed with culture medium alone and culture medium and solvent (this was prepared using water as solvent). 2 ml of each solution was transferred to each well and the plates were cultured in a humidified atmosphere at 5%CO_2 and 37ºC for 21 days. Twice a week, 200 µL of RPMI-1640 culture medium supplemented with 10% (v/v) of FBS was added to each well. After this period the number of visible colonies was counted visually.

The results were expressed in plate efficiency, which accounts for the ratio of number of colonies counted and the total cell number inoculated in each well:

$$Plate\ efficiency\ (\%) = \frac{number\ of\ colonies}{total\ cell\ number} \times\ 100 \qquad (3)$$

This result was normalized relative to the control. This assay was performed with duplicates for each condition in, at least, 5 independent experiments.

2.10. Gene expression analysis

2.10.1. RNA Extraction

This assay was performed in order to evaluate the variations in the genetic expression of the spheroid's cells when exposed to the tested compounds. For do so, 50 spheroids were collected to each well of a 6-well plate and 2 mL of RPMI +0.5% (v/v) FBS with the compounds to test in the desired concentration was added to each well. For this assay, only HT was tested, for the concentrations of 200 µM and 600 µM. The controls with culture medium and the solvent (miliQ water) were also tested. After a 72h incubation period, the spheroids were transferred to an eppendorf and centrifuged for 5 min at 200g. The supernatant was removed and the cellular lysis was accomplished by adding 600 µL of lysis buffer RTL (QIAGEN, Hilden, Germany) with 1% (v/v) of β-mercaptoetanol and with the help of mechanic dissociation with a syringe. The samples were stored at -80ºC until RNA extraction and its analysis in the Portuguese Institute of Oncology.[50,52,54,70]

After thawing samples on ice, it was added 600 µL of 70% (v/v) Ethanol in DEPC-treated water to each eppendorf sample (total volume of 1200 µL), in order to inhibit the degradation of the RNA. 700 µL of this sample were transferred to a RNeasy® Mini spin column (QIAGEN, Hilden, Germany) placed in a 2 mL collection tube and it was centrifuged at 14.000 rpm for 30 seconds. The supernatant was removed and the previous step was repeated with the remaining 500 µL of each sample, reusing the same RNeasy Mini spin column and collection tube. After, the spin column was washed with 700 µL of RW1 buffer and centrifuged at 14.000 rpm for 30 seconds. After discarding the flow-through of the collection tube, 500 µL of RPE buffer were added to the spin column, repeating the above-mentioned step of centrifugation. The supernatant was removed from the collection tube and the washing step with RPE buffer was repeated followed by a centrifugation at 14.000 rpm for 2 minutes. The spin column was placed on a new collection tube and it was centrifuged again for 1 minute at 14.000 rpm to remove residual RPE buffer or supernatant still on the outside of the column. Afterwards, to perform RNA elution, the spin columns were placed in 1.5 mL eppendorfs and it was added 40 µL of RNAse-free water to each column membrane followed by another centrifugation at 14.000 rpm for 1 minute. The samples were kept on ice.[51,52]

The total RNA concentration was quantified by ultraviolet spectrophotometry at 260 nm with a Nanodrop 2000 Spectrophotometer (Thermo Scientific), considering that an absorbance reading of 1 at 260nm corresponds to approximately 40 µg/mL of RNA. Total RNA samples were stored at -80 ºC until further use.[51,52]

2.10.2. cDNA synthesis

The previously obtained RNA samples were used as a template for the complementary DNA (cDNA) by a reverse transcriptase enzyme, using reagents from Invitrogen (USA). This step

was accomplished using random primers that hybridize with messenger RNA templates and nucleotides for DNA synthesis (dNTPs). Approximately 1000ng of total RNA were transcribed into cDNA in a final reaction volume of 20 μL with a final concentration of 50ng/μL. Briefly, in 0.2ml reaction tubes, it was added the volume of total RNA corresponding to 1000ng, 0.5μL of random primers and the necessary amount of DEPC-treated nuclease-free water to make up the final volume of 7.75 μL. This solution was incubated for 10 minutes in a T3 Thermocycler (Biometra) and put on ice afterwards. It was added to the samples 12.25μL of a master mix composed of 4μL 5x First Strand Buffer (Invitrogen), 4μL of dNTPs, 2μL of DTT (Invitrogen), 0.75μL of RNase Out Recombinant Ribonuclease inhibitor 5.000U (40U/ μL;Invitrogen), 1 μL of Superscript II Reverse Transcriptase 10.000U (200U/ μL; Invitrogen) and 0.5 μL of DEPC-treated nuclease-free water. Afterwards the reverse transcription was carried out at 42ºC for 1 hour and the reaction was stopped by heating to 70ºC for 10 minutes. The cDNA samples were stored at -20ºC until further use.

2.10.3. Quantitative reverse transcription-polymerase chain reaction (RT-qPCR)

This assay allows for the quantification of the expression of targeted genes. In this process, each reaction cycle includes a melting phase with the separation of the double stranded cDNA with high temperature, followed by an annealing phase with the primer binding to the DNA templates and finally the polymerization phase accomplished by a DNA polymerase enzyme at a lower temperature. During this last phase, each DNA base that is incorporated to the growing chain is marked with a fluorophore (SYBR Green I fluorescence probe) and the detection of the DNA quantity during the exponential phase of the nucleic acid amplification is accomplished by the measurement of the intensity of the fluorescent signal emitted upon the annealing. Therefore, this technique allows for the qualitative and quantitative analysis of DNA, being the quantification relative once it is calculated by normalizing data using an endogenous gene control – HRPT1. The fluorescence measurement is made above a given threshold (which excludes the background signal) and the number of cycles required for each sample to reach the threshold fluorescence is designated CT value. Therefore, samples in which a target gene has increased expression, will reach the threshold value faster than samples in which the target gene is less expressed (lower CT value).

Briefly, 2 μL of the previously obtained cDNA was amplified with Power SYBR® Green Quantitative PCR MasterMix (Applied Biosystems, CA, USA) or Kapa SYBR® Fast Universal qPCR kit (Kapa Byosistems, MA, USA) according to the optimal conditions for each primer. All the PCR reactions were carried out in PCR 96-Microwell plates (Axygen Scientific) in a final volume of 15 μL and the experiment was performed in triplicates. For each sample, the master mix was prepared to a final volume of 13 μL as listed on table 4.

Table 4 – Components for the preparation of the qPCR Master Mixes.

Gene (marker)	Primer concentration (pmol/ µL)	Reaction Master Mix		
		Primer Volume	Mix	Water
HRPT1	7.5	0.75 µL of reverse primer + 0.75 µL of forward primer	7.5 µL of SYBR® Green PCR Master Mix (Applied Biosystems)	4 µL
CTNNB1 (β-Catenin)	5			
LGR5	7.5			
AXIN2	3.5			
NANOG	5			
OCT4	5			
CDKN1A	5		7.5 µL of SYBR® Green PCR Master Mix (Applied Biosystems)	4µL
VIM	5			
CDH1 (Cadherine)	5			
PTCH1	5			
TGFB1	3			
CCNA2 (Cyclin A2)	5		7.5 µL of Kapasyber® Fast qPCR Master Mix (2x) (Kapa Biosystems) + 0.3 µL of Kapasyber® Fast Rox High (50x) (Kapa Biosystems)	3.7 µL
GLI1	3			

After adding 13 µL of the mix to each corresponding well, 2 µL of cDNA were added to the respective well and the plate was sealed with PlateMax ultra-clear sealing film (Corning Axygen). Afterwards the plate was centrifuged for 1 minute at 1200rpm. Finally, the qPCR reactions were carried out in ABI PRISM 7000 Sequence Detection System (Applied Biosystems) and monitored in SDS Software (Applied Biosystems). The thermal cycling comprised the following steps: initial denaturation at 50ºC for 2 min followed by 10 minutes at 95 ºC, then the PCR stage takes place with 40 cycles of denaturation and annealing at 95ºC for 15 seconds followed by 1 minute at 60ºC, and lastly a dissociation stage at 95ºC for 15 seconds followed by 60ºC for 1 minute.

All the data collected was normalized to the expression levels detected for HRPT1, subsequently normalized relatively to the solvent control. Several endogenous controls were tested, namely: GAPDH, β-actin, 18S and HRPT1. However the difference between CTs of different conditions (control + solvent and HT 600 µM) for *GAPDH, β-actin* and *18S* were over 0.7 units, reaching, in some cases, 1.5 units of difference. Normally, the ideal maximum difference between different condition's CT must be under 0.5 in order to ensure that the compound does not modulate the endogenous gene control. The only one that fulfilled this condition was HPRT1. Even though the maximum difference observed was 0.6, it was the

most suitable control found. Therefore, and after several repetitions of this assay, only one independent experiment (n) was yielded from it, since this study was performed on another lab and with a limited amount of time available.

2.11. Statistical analysis

Statistical analysis of the results was performed using GraphPad Prism 6 software (GraphPad Software, Inc., CA). Comparisons between samples were made by One-way ANOVA analysis. Comparisons with more than two variables were performed by a Two-way ANOVA analysis. Both types of statistical analysis followed Tukey's multiple comparison tests. Values of $p<0.05$ were considered statistically insignificant.

3. Results and Discussion

3.1. Antiproliferative effect and cytotoxicity evaluation of hydroxytyrosol and its colonic metabolites - 2D cell models

Aiming at assessing the antiproliferative effect of HT, PA and PPA on colorectal cancer cells, the HT29 cell line was used as a 2D cell model (in monolayer). These cells were incubated with the tested compounds for 72 hours, with several concentrations (from 25 to 400 μM) in order to assess the dose-dependent response effect in cell proliferation. Results are shown in Figure 17.

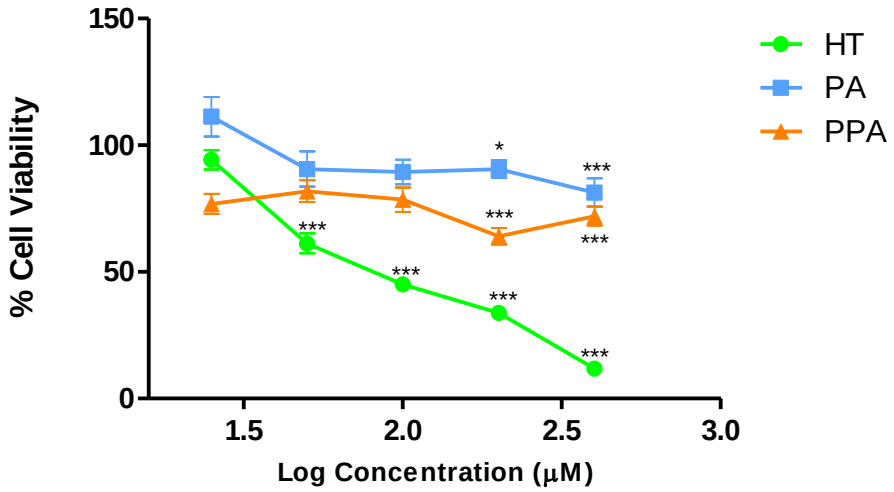

Figure 17 – Dose response profiles of the antiproliferative effect of HT, PA and PPA after a 72h period of incubation on HT29 cell monolayer. The results are expressed as mean ± standard deviation of 3 independent assays, each of them performed in triplicates. *p-value < 0.05, **p-value <0.01 and ***p-value < 0.0001 are relative to the control.

Results showed significant differences for the three compounds, which were tested under the same conditions and for equal concentrations. It is clearly noticeable that HT presented an antiproliferative effect in a dose dependent manner with an EC_{50} of 93.58 μM. The same effect was not observed for the PA and PPA compounds. As shown in Figure 17, PA and PPA presented a lower antiproliferative effect. PPA causes a decrease in cell viability for almost all the concentrations tested, being the cell viability around 70%. However, no dose-response dependency was observed for this compound. Regarding PA, a slightly dose-response tendency was obtained, as cell viability drops to around 75%-80% for concentrations above 50 μM

The antiproliferative effects of HT are already reported in the literature, not only in colon cancer cell lines, but also in hepatoma, breast and prostate cancer cell lines. [71–74] Previous studies had already reported the antiproliferative effect of HT using concentrations of 100 μM in HT29 cell line.[43] On this same study, it was shown that HT and PA produce cell cycle arrest and promote apoptosis for that same concentration.[43] Juan et al also reported an EC_{50} of 58.5 ± 2.7 μM for a 2D antiproliferative assay using HT29 cell line, result that is relatively

comparable to the one obtained in the present study.[62] Additionally Terzuoli et al also reported the reduction of CRC growth caused by HT, achieving an EC_{50} value of 181.8 μM (almost two times higher than the EC_{50} value obtained in this study).[64] However it is important to note that this difference in EC_{50} values can be explained by the different cellular concentrations used in the inoculum.

In order to evaluate if the tested concentrations were toxic to the normal epithelium, cytotoxicity studies were performed on confluent Caco-2 cell line. This cell model shares some characteristics with crypt enterocytes and is considered a widely accepted model to study the effect of drugs and food compounds on intestinal function.[75] The concentrations tested ranged from 125 μM to 2000 μM and the results of this assay are demonstrated on figure 18, presented on a logarithmic scale.

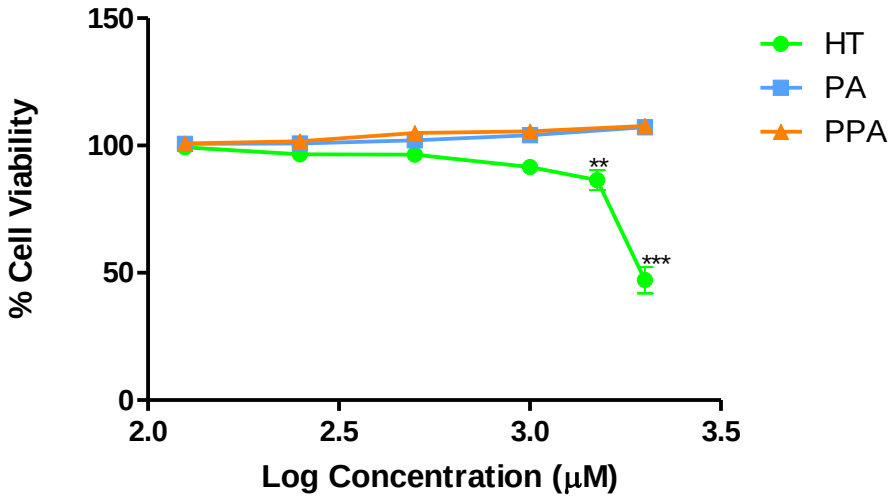

Figure 18 - Cytotoxicity effect of HT, PA and PPA on a 2D cell model of intestinal barrier. Dose-response profiles of cytotoxic effect provoked by HT, PA and PPA compounds after a period of incubation of 72 hours in Caco-2 cell line. Green represents hydroxytyrosol, blue represents phenylacetic acid and orange represents phenylpropionic acid. The results shown here are the mean of 5 independent experiments, each one performed with triplicates ± SD. **p-value < 0.01 and ***p-value < 0.0001 are relative to the control.

As it can be seen in figure 18, PA and PPA did not cause any cytotoxic effect for any of the concentrations tested. On the other hand, HT significantly decreased cell viability relative to the control for the higher concentrations tested (1000 and 2000 μM). The calculated IC_{50} value for HT was 1971.0 μM. Importantly, since the EC_{50} of the antiproliferative assay is lower than the IC_{50} determined in Caco-2 cells it can be suggested that HT inhibits colorectal cancer cell growth without compromising the viability of normal colon cells. In fact the cytotoxicity of HT has been widely studied not only in Caco-2 cell lines as well as other cell lines. In the future, it would be of interest to perform this same cytotoxicity assay in an original colon epithelium cell line like the CCD 841 CoN.

In vivo toxicity studies were already performed in mice.[76] Results showed that the ingestion of HT up to 50 mg/kg of body weight per day had no observed adverse effect level. The

European Food Safety Authority (EFSA) considered hydroxytyrosol as a novel food and the FDA set a maximum daily intake of this pure synthetic hydroxytyrosol of 51.06 mg/person (0.85 mg/kg body weight per day).[76,77]

It is important to mention that a daily consumption of 33 g of olive oil would result in an estimated intake of about 0.5mg of hydroxytyrosol per day. It is estimated that, in the Mediterranean countries, the mean intake of hydroxytyrosol lies at 31 mg (through the consumption of olives and olive oil), a value considerably lower than the maximum dosages mentioned before. [62]

3.2. Antiproliferative effect of hydroxytyrosol and its colonic metabolites using a 3D model for colorectal cancer

The anticancer properties of hydroxytyrosol on colorectal cancer have been widely studied on 2D cell models, showing a clear antiproliferative and antiapoptotic effect. [63] However for 3D cell models there is a lack of information on the effects of HT and its colonic metabolites.

Besides evaluating the antiproliferative activity of hydroxytyrosol and its colonic metabolites on a 2D cell model, and taking into consideration the importance of a cell model that better mimics the *in vivo* tumor heterogeneity, an antiproliferative assay on the 3D cell model of HT29 cells was performed. For this purpose, HT29 cell spheroids, obtained by culturing these cells on a stirred cultured system, were used to evaluate the bioactive effect of VOO metabolites. As described previously, spheroids collected on day 7/8 of culture present features of in vivo solid tumors, such as cell-cell and cell-ECM interactions, hypoxia, oxygen, nutrient and waste gradients, drug penetration, response and resistance, production and deposition of ECM, among others. Therefore, in this work, the spheroids collected at this time point were collected and incubated with HT, PA and PPA to assess their antiproliferative effect. In figures 19 and 20 is presented the dose-response profiles of HT and its colonic metabolites, respectively.

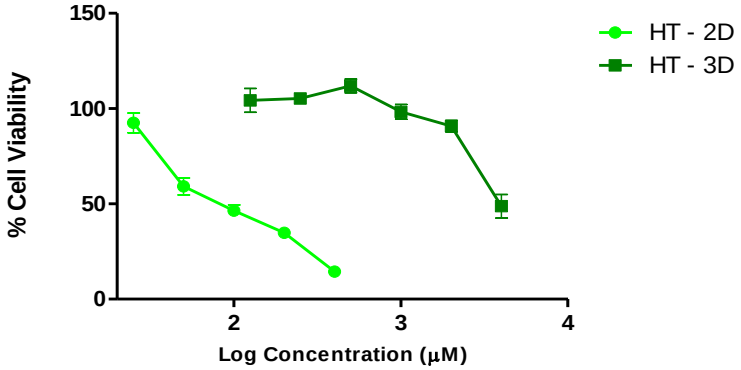

Figure 19 – Antiproliferative effect of Hydroxtyrosol on the 2D and 3D cell models of colorectal cancer using the HT29 cell line and with an incubation period of 72 hours. In light green is represented the curve response for the HT using the 2D cell model and in dark green the curve for the 3D cell model. Results are expressed in mean of 4 independent experiments performed in triplicates for the 2D and 2 independent experiments with six replicates for the 3D ± SD.

The HT concentrations tested for the 3D antiproliferative assay ranged from 125 to 4000 µM. Figure 19shows an antiproliferative effect of HT on the 3D cell model, being clearly visible by the profile of the curve that this compound inhibited cell proliferation in a dose-dependent manner. The calculated EC_{50} for the 3D cell model was 3938 µM.

Comparing the results obtained in both antiproliferative assays it is possible to verify that the EC_{50} obtained for the 3D assay is 42 times higher than the 2D one. This fact can be explained by the physiological differences between the 2 cell models. The higher concentration of HT necessary to reduce 50% of the cell viability in 3D spheroids can be explained by several factors: i) Diffusional limitations - there is a higher cell concentration within the spheroid, hampering the diffusion of the compound to all the HT29 cells of the spheroid; ii) structural complexity of HT29 cell spheroids: the population of cells in the spheroid is not homogeneous, existing, proliferating cells, quiescent cells, necrotic cells and cancer stem cells within the tumor, all of whom with different characteristics; iii) chemoresistant phenotype of HT29 cell spheroids: the colon cancers are fundamentally resilient to treatments because of radio and chemotherapy resistance by several mechanisms - the stochastic selection of resistant genetic subclones, microenvironmental factors (hypoxia, acidosis) and other extrinsic cellular factors, as well as the existence of CSC that are highly resistant. [78,79] All of this factors are better mimicked in a 3D cell model than in a monolayer (2D) one.[78,79]

The same discrepancy between the results of EC_{50} values obtained for 2D and 3D cultures have already been reported on previous studies of the same host lab, with other food matrices and bioactive compounds such as *brassicaceae* extracts, isothyocyanates, citrus fruit extracts and polymethoxylated flavones.[50,54] As reported above, this effect was justified by the fact that the spheroids collected on the day 7 of culture display characteristics observed in *in vivo* carcinomas: hypoxic regions, apoptotic/necrotic core, presence of cancer stem cells and less differentiated cells in the surrounding area which confers the said chemoresistance.[53,54] This is supported by evidence of an increase in stemness markers and on the percentage of ALDH+ cells of the 3D cell model, when compared to monolayer.[54] Evidence also suggests that the 3D cell model presents a more mesenchymal and migratory tumor cell phenotype than the monolayer culture. [54] All this data supports the results obtained and the discrepancy in the values yielded for the 2D and 3D cell cultures for some food bioactive compounds.

The colonic metabolites of HT – PA and PPA – were also tested on the 3D cell model. The dose-response profile of this assay is shown in figure 20.

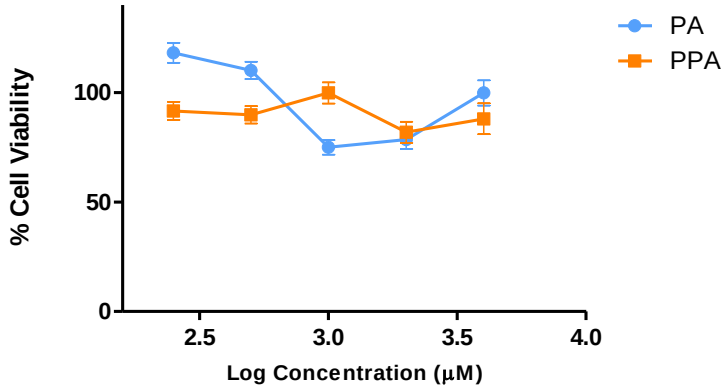

Figure 20 - Antiproliferative effect of PA and PPA on the 3D cell model of colorectal cancer using the HT29 cell line and with an incubation period of 72 hours. In blue is represented the curve response for the PA and in orange the curve response for the PPA. Results are expressed in mean of 3 independent experiments performed with six replicates for the 3D ± SD.

As it is shown on figure 20, neither PA nor PPA inhibited cell proliferation in HT29 cell line spheroids.

From the results obtained for all the compounds tested, the only compound that exerted some antiproliferative effect was HT. This compound demonstrated the ability to inhibit the growth of the HT29 cells using the model of the disease that better mimics human tumors. However, it is important to mention that the EC_{50} value is within the cytotoxic range obtained in Caco-2 cell line assays. Future studies should be performed in order to validate the safety of HT in normal colon call line.

3.3. Inhibition of aldehyde dehydrogenase activity (Aldefluor assay)

One of the key factors for the success of the treatment of colorectal cancer is the targeting and elimination of the cancer stem cells. In order to determine whether HT and its colonic metabolites PA and PPA have the potential to counteract the detoxifying action of ALDH1 or decrease its activity, the Aldefluor assay was carried out using flow cytometry.

This assay was performed with the goal of understanding the influence of hydroxytyrosol and its colonic metabolites in the stemness of the HT29 spheroids (particularly in the $ALDH^+$ population). The results of this assay are presented in figure 21.

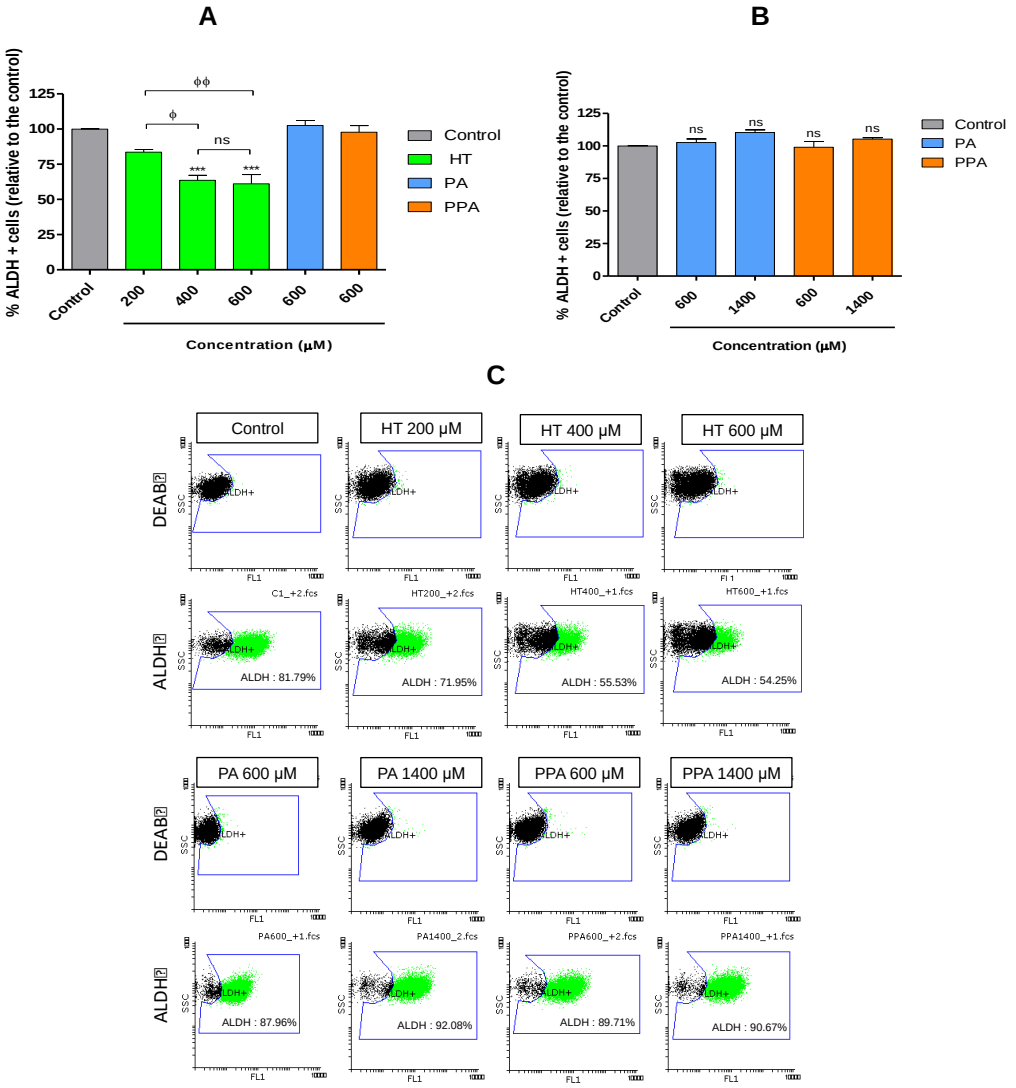

Figure 21 – (A) Effect of HT, PA and PPA on the population of ALDH⁺ cells. The results are shown in mean of 4 independent experiments, each one performed with duplicates, ± SD. (B) **Effect of higher dosages of PA and PPA on the population of ALDH⁺ cells.** The results are shown in mean of 3 independent experiments, each one performed with duplicates, ± SD. (C) **Representative dot plots of ALDH1 subpopulation in HT29 spheroids from flow cytometry analysis using ALDEFLUOR™ assay.** . ***p-value < 0.0001 is relative to the control and ns (p-value>0.05), ϕp-value<0.05 and ϕϕp-value<0.01 are relative to the same compound.

As shown in figure 21 (A), there was an effect of HT causing the decrease of ALDH⁺ cells in a dose-dependent way: for the concentration of 200 µM the mean percentage of ALDH⁺ cells is 83.6% (reduction of 16.4% relative to the control), for the 400 µM the mean percentage is 63.6% (reduction of 36.4% relative to the control) and for 600 µM the percentage of ALDH⁺ cells is 61% (reduction of 39% relative to control). Between these two highest dosages, there was not a statistically significant difference, suggesting that this increase on the concentration is not enough to cause a decrease on the population of ALDH⁺.

In order to determine whether PA and PPA could have a potential activity on inhibiting the ALDH1, a higher concentration was tested and the results are shown in figure 21 (B). Even for higher concentrations, PA and PPA did not show any effect on the reduction of the population of ALDH⁺ cells.

Aldehyde dehydrogenase activity has been associated with the stemness characteristics of tumors. Colorectal cancer exhibits ALDH activity, being its activity significantly higher in cancer tissues than in healthy ones (about 27-29%).[80] Hydroxytyrosol, as well as other phenols present in VOO, have shown to be able to reduce the $ALDH^+$ population in breast cancer cell lines.[81,82] Accordingly to Cruz-Lozano et al, HT reduced the breast cancer stem cells self renewal and ALDH+ subpopulation: concentrations of 25, 50 and 75 μM were tested during an incubation period of 4 days in three different 2D breast cancer cell lines, yielding in a reduction of up to 90% relative to the control.[81] Nonetheless it is important to notice that in this last study the percentage of $ALDH^+$ cells in the control were fairly low (<5.86%).[81] Additionally, Corominas-Faja et al reported that oleuropein (oleuropein is the precursor of HT) is able to selectively target subpopulations of epithelial-like $ALDH^+$ and mesenchymal-like CSC in breast cancer cell lines.[82]

In this work, it is clear a reduction in the $ALDH^+$ subpopulation of cells caused by HT. This result is of great importance since targeting and reducing the population of cancer stem cells is a big hallmark in the fight against CRC and in inhibiting the progression of this disease to metastasization. Further work would be of great importance to test other CSC markers to attest for the results here obtained with the ALDH.

3.4. Assessment of anchorage-independent cell growth

The technique of this assay – Colony Forming Unit assay (CFU) – is widely used to evaluate cellular transformation *in vivo*: while normal cells are prevented from anchorage-independent growth due to a particular type of apoptotic death called anoikis, transformed cells have the capability to grow and divide without binding to a substrate.[83] Anoikis prevents detached epithelial cells from colonizing elsewhere and is an essential mechanism for tissue homeostasis and development. An anchorage-independent growth and EMT are two of the features associated with anoikis resistance, tumor progression and metastatic spreading of cancer cells.[83–85]

Normal cells depend on cell-ECM contact to be able to grow and divide, and on the other hand, transformed cells have the ability to grow and divide independently of their surrounding environment, forming colonies in an anchorage-independent way. The cells that posse this ability are considered to be transformed and carcinogenic. Moreover, anchorage independent cell growth alongside with self renewal ability constitute some of the main characteristics associated with CSCs. [83,86]

In order to evaluate the effect of HT and its colonic metabolites in preventing anchorage-independent cell growth, soft agar assay was performed (as described in section 2.9). This assay allowed exploring the ability of cells to form colonies from a single cell in a semi-solid support, given by agarose. For that, HT29 spheroids were collected on day 7 of culture and enzymatically dissociated into single cells and plated on an agarose semi-solid matrix gel. The compounds were then incubated on the wells for 72h: HT at concentrations 5, 10, 20 and

50 µM and PA and PPA at concentrations 20, 200 and 500 µM. The results of this assay are shown in figure 22.

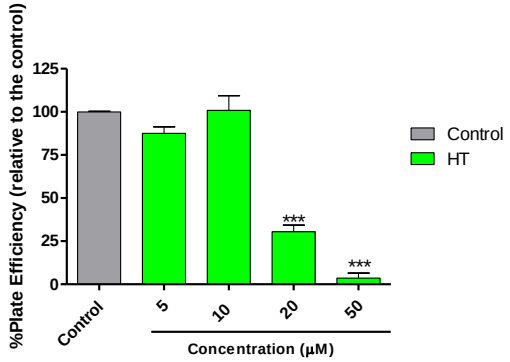

Figure 22 – Plate efficiency for the anchorage-independent cell growth using cells derived from HT29 spheroids, treated with HT for a timespan of 3 weeks. The value of the plate efficiency was calculated recurring to equation 3, which expresses the percentage of single cells that gave rise to a colony unit. Therefore, the lower plate efficiency translates into a higher inhibitory effect by the compound. Results are mean of 5 independent experiments performed in duplicates ± SD. ***p-value<0.001 is relative to the control.

The range of dosages tested were considerably lower to the EC_{50} concentration obtained for the same compounds which is justified by: i) lower cell density per well; ii) increased susceptibility to the compounds of the single cells seeded in agar. Results showed that HT promoted an inhibition of colony formation in a dose dependent-manner, with an almost total inhibition for the highest concentration tested (96.4% for 50 µM) and a mean reduction on the plate efficiency of 70% for HT 20 µM. These results demonstrate that with a higher concentration, the anti-tumorigenic potential of HT compound becomes more accentuated. It is important to refer that, although not statistically significant, the concentration of 10 µM appears to lead to a slight increase of the plate efficiency, however, the observation of the colonies of this concentration after the 3 weeks of culture, revealed that they were considerably smaller and less compact than the ones formed in the control and 5 µM HT wells.The colonic metabolites of HT (PA and PPA) were also tested and the results are shown on figure 23.

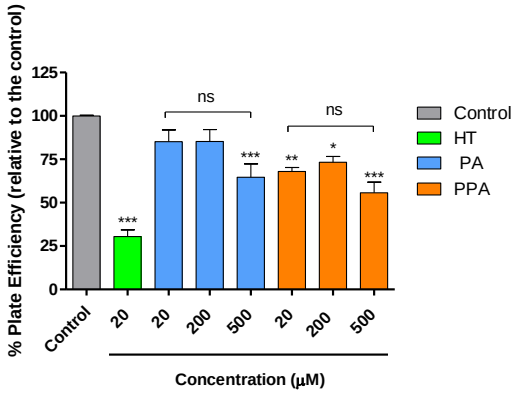

Figure 23 - Plate efficiency for the anchorage-independent cell growth using cells derived from HT29 spheroids, treated with HT, PA and PPA for a timespan of 3 weeks. The value of the plate efficiency was calculated recurring to equation 3, which expresses the percentage of single cells that gave rise to a colony unit. Therefore, the lower plate efficiency translates into a higher inhibitory effect by the compound. Results are mean of 5 independent experiments performed in duplicates ± SD. *p-value < 0.05, **p-value <0.01 and ***p-value < 0.0001 are relative to the control and ns (p-value > 0.05) is relative to the same compound.

The results showed that PA and PPA did not present the same inhibitory effect as HT. In fact, PA only showed a significant inhibition of colony formation for the higher concentration (500 µM), where the mean reduction was 35%. Even though this result is statistically different from the control, it is not statistically different from other concentrations tested of the same compound, namely 20 and 200µM. As for PPA, all of the concentrations tested, from 20, 200 and 500 µM, showed significant reductions in colony formation, approximately between 27% to 44% relative to the control.

Up to date, there are no studies reporting the effect of HT and its colonic metabolites in reducing colony formation of CRC cells. Only Terzuoli et al also showed that HT at 10 µM when combined with a chemotherapeutic drug - cetuximab (1 µg/ml) - improve the action of this compound in inhibiting the colony formation using HT29 and WiDr cell lines.[87] Similar studies with other extracts had already been performed and the range of concentrations tested that showed to be efficient in colony formation inhibition are similar to the ones tested for HT, PA and PPA. In particular, *Brassicaceae* extracts and citrus peels extracts enrich in isothyocyanates and polymethoxylated flavones, respectively, had already reported to inhibit colony formation in HT29 cell spheroids: 5 µM of sulforaphane enrich-broccoli extract almost completely abolished the tumorigenic potential of spheroid-derived cells (3.3% relative to the control), whereas 20 to 60 µM of polymethoxylated flavones, in particular tangeritin, showed reductions up to 95% relative to the control.[50,54]

Taken together, the results obtained from this assay suggest that among all compounds, hydroxytyrosol might have a potential role in targeting colorectal CSCs.

3.5. Combination of hydroxytyrosol and 5-fluororacil

5-Fluororacil (5-FU) is a fluorinated pyrimidine, one of the most widely used agents for the treatment of colon cancer. As a matter of fact, no other agent has proved more effective as a first-line of therapy in more than 40 years that this drug has been available.[39] However, despite its widespread use, the cytotoxicity of 5-FU is not limited to tumor tissue, with hematopoietic and normal epithelial cells in the gastrointestinal tract being susceptible to its toxicity. [39]

The need to improve the survival of patients with metastatic colon cancer has led to the development of combination therapies.[39] In this study, the effect of the combination of HT with 5-FU was studied in order to assess the potential effect of this natural compound in improving the efficacy of the drug, in terms of antiproliferative response, inhibition of anchorage independent cell growth and reduction of the subpopulation of $ALDH^+$ cells (Figure 24).

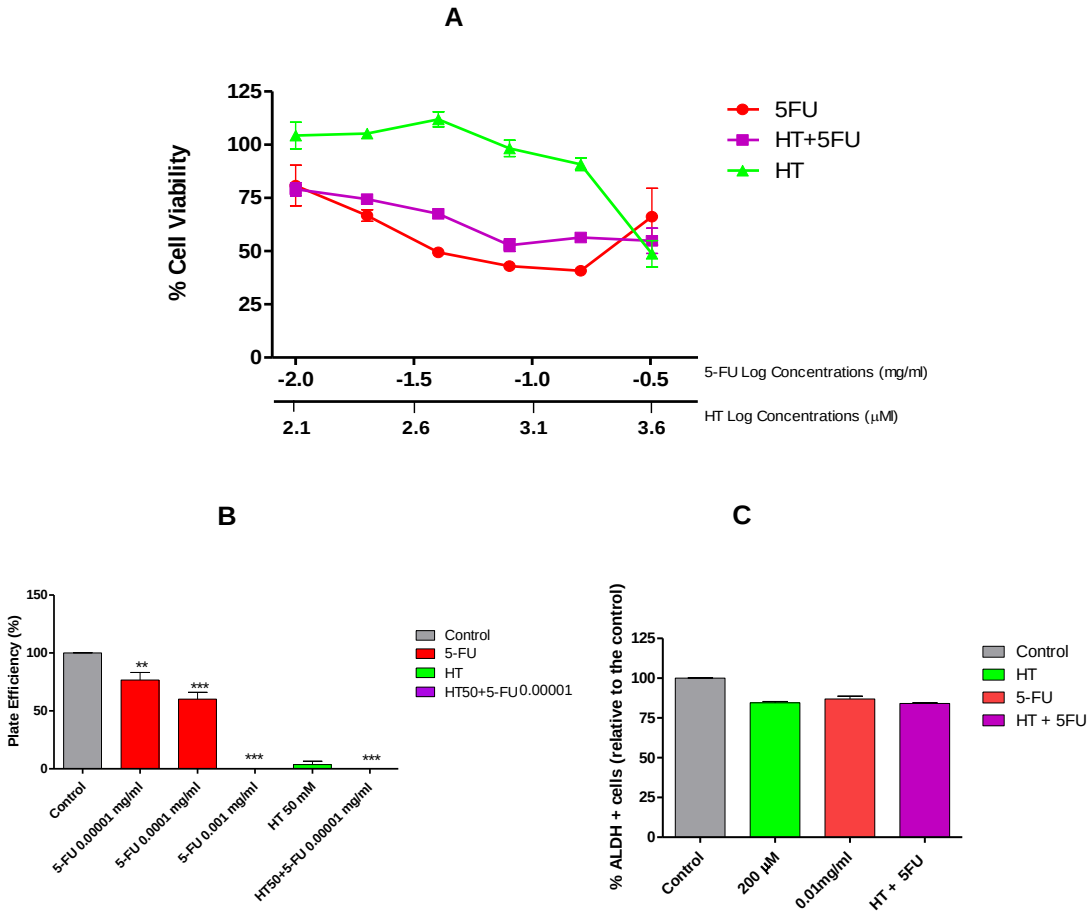

Figure 24 – (A) Antiproliferative effect of Hydroxtyrosol, 5-fluororacil and the combination of the two compounds on the 3D cell model of colorectal cancer using the HT29 cell line and with an incubation period of 72 hours. Results are expressed in mean of, at least, 2 independent experiments performed with 6 replicates. (B) **– Plate efficiency for the anchorage-independent cell growth using cells derived from HT29 spheroids, treated with 5-fluororacil and a combination of 5-FU and HT for a timespan of 3 weeks.** The value of the plate efficiency was calculated recurring to equation 3, which expresses the percentage of single cells that gave rise to a colony unit. Therefore, the lower plate efficiency translates into a higher inhibitory effect by the compound. (C) **Effect of HT, 5-fluororacil and the combination of both compounds on the population of ALDH$^+$ cells.**

From the results obtained from the antiproliferative assay testing the combination of HT and 5-FU, shown in figure 24 (A), it is possible to observe that the EC_{50} value of the combination of the compounds, HT and 5-FU (0.3 mg/ml of 5-FU) was singly higher than the EC_{50} of 5-FU alone (0.13 mg/ml). Therefore, HT did not improve the antiproliferative effect of 5-FU in HT29-cell spheroids.

For colony forming units assay, 3 concentrations of 5-FU were tested: 0.001, 0.0001 and 0.00001 mg/ml. The highest concentration tested completely inhibited the formation of colonies and the lower showed a plate efficiency of over 60%, clearly presenting a dose-dependent response (Figure 24B). A combination study was performed for this assay with the less concentrated dose of 5-FU and with HT 50 µM and results showed a total inhibition of colony formation for this combination. This result may indicate a synergetic effect between these two compounds, since HT 50 µM presented a mean of 4% plate efficiency. Nevertheless, to further assess this possibility, less concentrated dosages of HT should be tested in combination with 5-FU.

Finally, for the ALDH assay, it is clear that the percentage or $ALDH^+$ cells did not suffer a decrease for the combination of HT and 5-FU when compared to the compounds alone - the percentages of ALDH+ cells ranged between 84% and 86% (Figure 27C). Therefore, it is possible to conclude that no synergetic effect was observed for this combination. Further studies, with other concentrations of HT and 5-FU should be performed in order to confirm the effect of the VOO compound (HT) with this chemotherapeutic drug in targeting ALDH+ cells.

As mentioned before, combination studies were already performed using HT: Terzuoli et al performed a combination study with HT and cetuximab.[87] This is a monoclonal antibody that acts as an epidermal growth factor receptor inhibitor and enhances antitumor effects of chemotherapy and radiotherapy by inhibiting cell proliferation, angiogenesis and metastasis and by promoting apoptosis. [88] Results showed that the combination of HT - cetuximab was able to reduce cell growth in HT29 and WiDr cells at concentrations 10 times lower than when used as single agents. This combination was also able to reduce colony formation in both HT29 and WiDr cell lines.[87] Bernini et al synthetized a novel ester of HT and α-lipoic acid (a non-phenolic compound present mainly in wheat, potatoes and red meat).[89] This ester induced a significantly more potent cell growth inhibition at all dose levels compared with HT and α-lipoic acid either singularly or in combination. This novel compound attained an inhibition of tumor cell growth in HT29 cell-line of 69.6% with a concentration of 150 μM for an incubation period of 24h. HT achieved a comparable inhibitory effect with the double of the concentration (300 μM) for the same time period.[89] Another study also explored the effect of combining 5-FU with a natural product: hexahydrocurcumin, a major metabolite of *curcumin* with strong antioxidant activity.[90] Results concluded that this compound combined with a low dose of 5-FU exerted a synergistic effect against the growth of HT29 cells, markedly reducing cell viability to a greater degree than monotherapy.[90]

All this data suggests that combination therapies are a promising chemotherapeutic tool. Regarding HT, future studies should focus on combining this compound with other phenolic compounds or with other chemotherapeutic drugs that could possibly enhance its activity.[91] Multiple *in vivo* and *in vitro* studies have shown that mixtures of phenolic compounds more effectively inhibit tumor growth than the compounds employed singularly. Additionally, numerous in vitro and in vivo studies have also shown that polyphenols potentiate effects of conventional therapies and may help to reduce the effective dose of chemotherapeutic drugs, overcome drug resistance and reduce toxicities.[91] The development of nanotechnology to increase bioavailability and antitumoral activities of polyphenols can be a promising solution to overcome issues like the metabolism, stability, interference with other drugs and side effects of these natural compounds' derivatives.[91]

3.6. Influence of HT on the expression markers of cancer stemness, EMT, cell cycle and key signaling pathways

The influence of the treatments with HT on gene expression of key markers of cancer cell processes in the HT29 spheroids, collected at day 8, was evaluated by RT-qPCR. The aim of this study was to evaluate the influence of HT treatment on cancer stemness, EMT, tumor progression and major signaling pathways. For that, two concentrations used on the Aldefluor assay were chosen: 200 µM and 600 µM. The results obtained are shown in figure 25.

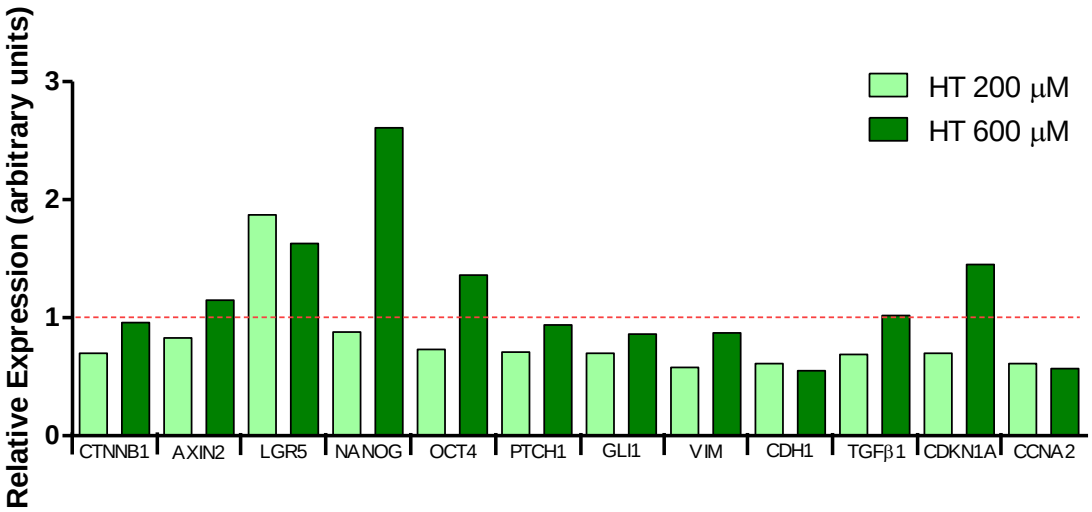

Figure 25 – Relative expression of specific markers using RT-qPCR for Wnt signaling (*CTNNB1, AXIN2*), stemness (*LGR5, NANOG, OCT4*), Sonic hedgehog pathway (*PTCH1, GLI1*), EMT (*VIM, CDH1*), and cell cycle (*TGFB1, CDKN1A, CCNA2*). The results were obtained using day 7 HT29 cell spheroids treated with HT at 2 concentrations for 72 hours. Each expression level was normalized relatively to the solvent control and the endogenous gene control used was HRPT1.

Analyzing the results obtained and shown on figure 25, the highest concentration tested (600 µM) did not appear to induce significant changes in the expression of cancer markers, with exception of the increase of the stemness markers (*LGR5, NANOG* and *OCT4*), as well as an increase of the *CDKN1A* and reduction of *CCNA2*, associated with cell cycle arrest.

Hence, these results hinder the antiproliferative ability of HT. However, considering the increase of the stemness markers, 600 µM is not a potentially promising concentration to pursue further studies. Nevertheless, dosages over 600 µM should be tested in further studies, since an increase of the stemness expression markers for this concentration, does not necessarily correspond to an increase of the same markers for higher concentrations.

Comparing the results obtained between the lowest (200 µM) and highest (600 µM) concentrations, generally there is an increase of the expression levels, more evident on the stemness markers, but also observed on the Wnt, Sonic Hedgehog pathway (SHH) and EMT, with an increase of *VIM*, *TGFβ1* and *CDKN1A*. However, for the lowest concentration tested

(200 μM), there seems to exist a slight reduction of the expression of almost all these markers, namely those related to stemness (*NANOG, OCT4*), EMT (*VIM*, *TGFβ1*) and SHH (*GLI1, PTCH1*), with the exception of the stemness marker and Wnt target gene *LGR5*. In terms of antiproliferative ability, this lowest concentration seems to have the opposite effect on the expression of *CDKN1A*, although a favorable effect in the expression of *CCNA2*.Therefore, a potential study of interest would be to combine HT 200 μM with a cytostatic drug.

Previous studies performed with HT on breast cancer cell lines have showed a dose-dependent reduction, among other, of β-catenin protein levels. This correlated to the inhibition of Wnt/β-catenin target genes. On this same study, it was observed a reduction of EMT-related transcription factors, which was correlated with a lower protein expression of the mesenchymal marker VIM. These results pointed to the inhibition of breast cancer stem cells self-renewal caused by HT, blocking the Wnt/ β-catenin signaling pathway and EMT. HT additionally showed to ablate the metastatic potential of tumor cells.[81] Another study revealed that HT reduces cell viability and induces dose-dependent apoptosis.[92] Even though these studies were performed on breast cancer cell lines and leukemia cells, the results obtained are still of great importance to the present study.

Although there is the need to repeat this assay in order to validate these results, as well as testing other dosages (below than 200 μM or even above 600 μM, closer to the EC_{50}, as long as it remains under the cytotoxic concentrations), it is possible to hypothesize that for smaller dosages, HT might have an anti-metastastatic effect (suggested by the reduction of *VIM, SHH, TGFβ1*, all involved in tumor invasion and metastasis, and also taken together with the inhibition effect obtained for the anchorage-independent assay). Even though the conclusions withdrawn can be seen as somewhat speculative, since only one independent study was performed, taken together with the results from already published studies, HT presents itself as a promising compound in inhibiting several mechanisms essential to cancer survival and metastasization.

From all the results obtained and described above it is possible to suggest that HT can be considered as a promising bioactive compound with potential applications in CRC prevention and therapy. In fact, there are already some clinical studies performed to assess the effect of this VOO compound against diseases like cancer and cardiovascular diseases. Currently there is an ongoing clinical trial for high-risk breast cancer prevention in women that consists in the ingestion of 25 mg of HT orally, everyday for one year.[93] The outcomes of this trial will be measured in two ways: mammographic breast density and the number of participants with adverse events. Other outcome measures will be the expression of Ki67 in tumor tissue and MRI breast density. [93] Importantly, some of the concentrations of HT tested in this work can be attained with a diet enriched in olive oil and olives. As reported previously the total mean daily intake provided by habitual consumption of olives and virgin olive oil is 31 mg of HT.[62]

According to Juan et al, if this phenol would reach the colon in a distribution volume of around 250ml, that would result in a concentration of approximately 72 μM a value that induced a 50% inhibition of cell proliferation in the same study.[62] Nevertheless it is important to mention that bioavailability studies have shown that HT is dose dependently absorbed in animals and humans after olive oil ingestion, while other phenolic components undergo metabolism in the small and large intestine.[94] In a study performed in humans, the absorption of pure hydroxytyrosol (99.5%) was investigated in the plasma and urine of healthy volunteers. HT was administered as a supplement in aqueous solution (2.5mg/kg body weight) and the absorption of HT was very low, and produced a large number of metabolites.[95] In the present study the colonic metabolites derived from HT, namely PA and PPA, showed lower inhibition of cancer cell proliferation and negligible effect on targeting cancer stemness than the native compounds. In future, other HT metabolites should be tested aiming at evaluating their potential anticancer activities.

As mentioned previously, the development of nanotechnology is a potent tool to increase bioavailability and antitumoral activities of polyphenols and can be a promising solution to overcome the abovementioned issues.[91]

4. Conclusion

Olive oil contains a vast range of substances such as monounsaturated free fatty acids, hydrocarbon, squalene, tocopherols, and phenolic compounds. Hydroxytyrosol is the most important phenolic compound in VOO, and presents several biological activities including anticancer effect. However, the molecular mechanisms underlying the protective action of HT against CRC are still unclear as well as its effect on cancer stem cell subpopulation.

In the present work, it was investigated for the first time the effect of the VOO compound hydroxytyrosol and its colonic metabolites phenylacetic acid and phenylpropionic acid in inhibiting proliferation and targeting cancer stemness on a 3D cell model of HT29 cells that better mimics and recapitulates the tumor microenvironment.

HT was the only compound able to reduce cell proliferation in this model of CRC, with an EC_{50} value of 3938 μM. Importantly, concentrations of 50 μM and 600 μM of HT showed to be effective in inhibiting anchorage-independent cell growth and decreasing in 39% the population of stem cells (ALDH+ cells), respectively. Furthermore it showed anti-metastasization potential by targeting specific gene expression markers, namely stemness markers (*NANOG, OCT4*), Epithelial to Mesenchymal Transition markers (*VIM*, *TGFβ1*), Sonic Hedgehog Pathway markers (*GLI1, PTCH1*) and proliferation markers (*CCNA2)*.

All together, the results obtained in this work suggest that HT presents a great potential as a chemotherapeutic adjuvant in order to more efficiently treat Colorectal Cancer, targeting and modulating CSC. Although combination studies with 5-FU revealed that HT does not significantly improve the antiproliferative response and the reduction of CSCs, the effect on inhibiting colony formation was improved indicating that this VOO compound can have a positive impact in chemotherapeutic impact of this conventional drug. More combination studies can also be performed with different chemotherapeutic drugs like oxaliplatin and irinocetan in order to assess the synergetic effect of HT.

In contrast, colonic metabolites derived from HT did not show antiproliferative effect and reduction of CSC population. These results indicate that the metabolization process of HT during gastrointestinal digestion process compromises the bioactivity towards CRC.

To better understand the beneficial effect of HT on CRC and cancer stem cells population, future studies can focus on evaluating the effect of different concentrations of HT on the Aldefluor assay as well as exploring other expression markers. Another future approach will rely on understanding the molecular mechanisms by which this compound inhibits CRC cell growth through omics platforms, such as metabolomics.

Bibliography

1. Bray, F. *et al.* Global cancer statistics 2018: GLOBOCAN estimates of incidence and mortality worldwide for 36 cancers in 185 countries. *CA. Cancer J. Clin.* **68**, 394–424 (2018).
2. Favoriti, P. *et al.* Worldwide burden of colorectal cancer: a review. *Updates Surg.* **68**, 7–11 (2016).
3. Union for International Cancer Control (UICC). GLOBOCAN 2018. Available at: https://www.uicc.org/new-global-cancer-data-globocan-2018#.
4. Wolf, A. M. D. *et al.* Colorectal cancer screening for average-risk adults: 2018 guideline update from the American Cancer Society. *CA. Cancer J. Clin.* **68**, 250–281 (2018).
5. Fanali, C. *et al. Cancer stem cells in colorectal cancer from pathogenesis to therapy : Controversies and perspectives*. **20**, (2014).
6. Thanikachalam, K. & Khan, G. Colorectal cancer and nutrition. *Nutrients* **11**, 255–262 (2019).
7. Cohn, S. M., Birnbaum, E. H. & Friel, C. M. Colon : anatomy and structural anomalies. 1369–1385 (2009).
8. Leslie, A., Carey, F. A., Pratt, N. R. & Steele, R. J. C. The colorectal adenoma-carcinoma sequence. 845–860 (2002).
9. Walther, A. *et al.* Genetic prognostic and predictive markers in colorectal cancer. (2011). doi:10.1038/nrc2645
10. Dexter, D. L. *et al.* Heterogeneity of Cancer Cells from a Single Human Colon Carcinoma. **71**, 949–956 (1981).
11. Kalluri, R. & Weinberg, R. A. Review series The basics of epithelial-mesenchymal transition. **119**, (2009).
12. Thompson, E. W., Newgreen, D. F., Thompson, E. W. & Newgreen, D. F. Carcinoma Invasion and Metastasis: A Role for Epithelial-Mesenchymal Transition? 5991–5995 (2005).
13. Weissman, I. L. Stem cells: Units of development, units of regeneration, and units in evolution. *Cell* **100**, 157–168 (2000).
14. Clarke, M. F. & Hass, A. T. *Cancer Stem Cells. Encyclopedia ofMolecular Cell Biology and Molecular Medicine, 2nd Edition* **568**, (2009).
15. Dean, M., Fojo, T. & Bates, S. Tumor Stem Cells And Drug Resistance. **5**, (2005).
16. Sagar, J., Chaib, B., Sales, K., Winslet, M. & Seifalian, A. Role of stem cells in cancer therapy and cancer stem cells: A review. *Cancer Cell Int.* **7**, 1–11 (2007).
17. Batlle, E. & Clevers, H. Cancer stem cells revisited. *Nat. Med.* **23**, 1124–1134 (2017).
18. Dalerba, P. *et al.* Phenotypic characterization of human colorectal cancer stem cells. *Proc. Natl. Acad. Sci.* **104**, 10158–10163 (2007).
19. Rodrigues, T. *et al.* Emerging tumor spheroids technologies for 3D in vitro cancer modeling. *Pharmacol. Ther.* (2017). doi:10.1016/j.pharmthera.2017.10.018
20. Chambers, A. F., Groom, A. C. & Macdonald, I. C. DISSEMINATION AND GROWTH OF. **2**, (2002).
21. Riihimaki, M., Hemminki, A., Sundquist, J. & Hemminki, K. Patterns of metastasis in colon and rectal cancer. *Sci. Rep.* **6**, 1–9 (2016).
22. Hanahan, D. & Weinberg, R. A. Hallmarks of Cancer : The Next Generation. *Cell* **144**, 646–674 (2011).
23. Todaro, M., Francipane, M. G., Medema, J. P. & Stassi, G. Colon Cancer Stem Cells : Promise of Targeted Therapy. *YGAST* **138**, 2151–2162 (2010).

24. Brabletz, T., Jung, A. & Kirchner, T. β -Catenin and the morphogenesis of colorectal cancer. 1–11 (2002). doi:10.1007/s00428-002-0642-9

25. Chu, P. *et al.* Characterization of a subpopulation of colon cancer cells with stem cell-like properties. **1321**, 1312–1321 (2009).

26. Yang, C. K. *et al.* Aldehyde dehydrogenase 1 (ALDH1) isoform expression and potential clinical implications in hepatocellular carcinoma. *PLoS One* **12**, 1–13 (2017).

27. Chen, J. *et al.* Prognostic Value of Cancer Stem Cell Marker ALDH1 Expression in Colorectal Cancer : A Systematic Review and Meta-Analysis. 1–15 (2015). doi:10.1371/journal.pone.0145164

28. Ma, I. & Allan, A. L. The Role of Human Aldehyde Dehydrogenase in Normal and Cancer Stem Cells. 292–306 (2011). doi:10.1007/s12015-010-9208-4

29. Baker, A., Graham, T. A., Elia, G., Wright, N. A. & Rodriguez-justo, M. Characterization of LGR5 stem cells in colorectal adenomas and carcinomas. 1–8 (2015). doi:10.1038/srep08654

30. Fanali, C. *et al.* Cancer stem cells in colorectal cancer from pathogenesis to therapy : Controversies and perspectives. **20**, 923–942 (2014).

31. Morgan, R. *et al. Wnt Signaling as a Therapeutic Target in Cancer and Metastasis*. *Introduction to Cancer Metastasis* (Elsevier Inc., 2016). doi:10.1016/B978-0-12-804003-4.00020-7

32. Novellasdemunt, L., Antas, P. & Li, V. S. W. Targeting Wnt signaling in colorectal cancer. A review in the theme: Cell signaling: Proteins, pathways and mechanisms. *Am. J. Physiol. - Cell Physiol.* **309**, C511–C521 (2015).

33. Fodde, R., Smits, R. & Clevers, H. APC, signal transduction and genetic instability in colorectal cancer. *Nat. Rev. Cancer* **1**, 55–67 (2001).

34. Colussi, D., Brandi, G., Bazzoli, F. & Ricciardiello, L. Molecular pathways involved in colorectal cancer: implications for disease behavior and prevention. *Int. J. Mol. Sci.* **14**, 16365–16385 (2013).

35. Taipale, J. & Beachy, P. A. The Hedgehog and Wnt signalling pathways in cancer. *Nature* **411**, 349–354 (2001).

36. Rimkus, T. K., Carpenter, R. L., Qasem, S., Chan, M. & Lo, H. W. Targeting the sonic hedgehog signaling pathway: Review of smoothened and GLI inhibitors. *Cancers (Basel).* **8**, 1–23 (2016).

37. Calon, A. *et al.* Dependency of Colorectal Cancer on a TGF-β-Driven Program in Stromal Cells for Metastasis Initiation. *Cancer Cell* **22**, 571–584 (2012).

38. Parnell, C. & Penella, J. W. Principles of cancer treatment by chemotherapy. (2003).

39. Prados, J. *et al.* Colon Cancer Therapy: Recent Developments in Nanomedicine to Improve the Efficacy of Conventional Chemotherapeutic Drugs. *Anticancer. Agents Med. Chem.* **13**, 1204–1216 (2013).

40. Ruiz De Porras, V. *et al.* Curcumin mediates oxaliplatin-acquired resistance reversion in colorectal cancer cell lines through modulation of CXC-Chemokine/NF-κB signalling pathway. *Sci. Rep.* **6**, 1–17 (2016).

41. Fuchs, C., Mitchell, E. P. & Hoff, P. M. Irinotecan in the treatment of colorectal cancer. *Cancer Treat. Rev.* **32**, 491–503 (2006).

42. Verjans, E., Doijen, J., Luyten, W., Landuyt, B. & Schoofs, L. Three-dimensional cell culture models for anticancer drug screening : worth the effort? *J. Cell. Physiol.* **233**, 2993–3003 (2017).

43. López De Las Hazas, M. C., Piñol, C., Macià, A. & Motilva, M. J. Hydroxytyrosol and the Colonic Metabolites Derived from Virgin Olive Oil Intake Induce Cell Cycle Arrest and Apoptosis in Colon Cancer Cells. *J. Agric. Food Chem.* **65**, 6467–6476 (2017).

44. Reya, T., Morrison, S. J., Clarke, M. F. & Weissman, I. L. Stem cells, cancer, and cancer stem

cells. *J. Clin. Rehabil. Tissue Eng. Res.* **11**, 2948–2951 (2007).

45. Breitenbach, M. & Hoffmann, J. Editorial : Cancer Models. **8**, 1–4 (2018).

46. Nyga, A., Cheema, U. & Loizidou, M. 3D tumour models : novel in vitro approaches to cancer studies. 239–248 (2011). doi:10.1007/s12079-011-0132-4

47. Zanoni, M. *et al.* 3D tumor spheroid models for in vitro therapeutic screening : a systematic approach to enhance the biological relevance of data obtained. *Nat. Publ. Gr.* 1–11 (2016). doi:10.1038/srep19103

48. Langhans, S. A. Three-Dimensional in Vitro Cell Culture Models in Drug Discovery and Drug Repositioning. **9**, 1–14 (2018).

49. Lin, R. Z. & Chang, H. Y. Recent advances in three-dimensional multicellular spheroid culture for biomedical research. *Biotechnol. J.* **3**, 1172–1184 (2008).

50. Pereira, L. P. *et al.* Targeting colorectal cancer proliferation, stemness and metastatic potential using Brassicaceae extracts enriched in isothiocyanates: A 3D cell model-based study. *Nutrients* **9**, 1–26 (2017).

51. Pereira, L. Exploring the chemotherapeutic potential of Brassicaceae extracts in colorectal cancer cell spheroids. (Faculdade de Ciências e Tecnologia (FCT), Universidade Nova de Lisboa, 2016).

52. Pereira, C. Effect of Citrus Bioactive Compounds on Targeting Human Colorectal Cancer Stem Cells (Master Dissertation). (Faculdade de Ciências e Tecnologia (FCT), Universidade Nova de Lisboa, 2016).

53. Silva, I. *et al.* Polymethoxylated Flavones from Orange Peels Inhibit Cell Proliferation in a 3D Cell Model of Human Colorectal Cancer. *Nutr. Cancer* **70**, 257–266 (2018).

54. Pereira, C. V *et al.* Polymethoxylated Flavones Target Cancer Stemness 5-Fluorouracil in a 3D Cell Model of Colorectal Cancer. (2019). doi:10.3390/nu11020326

55. Santo, V. E. *et al.* Adaptable stirred-tank culture strategies for large scale production of multicellular spheroid-based tumor cell models. *J. Biotechnol.* **221**, 118–129 (2016).

56. Gill, C. I. R. *et al.* Potential anti-cancer effects of virgin olive oil phenols on colorectal carcinogenesis models in vitro. *Int. Union Against Cancer* **7**, 1–7 (2005).

57. Hashim, Y. Z. H., Gill, C. I. R., Mcglynn, H. & Rowland, I. R. Components of Olive Oil and Chemoprevention of Colorectal Cancer. *Nutr. Rev.* **63**, 374–386 (2005).

58. Stark, A. H. & Madar, Z. Olive Oil as a Functional Food : Epidemiology and Nutritional Approaches. *Nutr. Rev.* **60**, 170–176 (2002).

59. Borzì, A. M. *et al.* Olive oil effects on colorectal cancer. *Nutrients* **11**, (2019).

60. Hull, W. E. *et al.* Olives and olive oil in cancer prevention. *Eur. J. Cancer Prev.* 319–326 (2004). doi:10.1097/01.cej.0000130221.19480.7e

61. Corona, G., Spencer, J. & Dessì, M. Extra virgin olive oil phenolics: absorption, metabolism, and biological activities in the GI tract. *Toxicol. Ind. Health* **25**, 285–293 (2009).

62. Emília Juan, M., Wenzel, U., Daniel, H. & Planas, J. M. *Cancer Chemopreventive Activity of Hydroxytyrosol: A Natural Antioxidant from Olives and Olive Oil*. *Olives and Olive Oil in Health and Disease Prevention* (Elsevier Inc., 2010). doi:10.1016/B978-0-12-374420-3.00144-3

63. Marković, A. K., Torić, J., Barbarić, M. & Brala, C. J. Hydroxytyrosol, tyrosol and derivatives and their potential effects on human health. *Molecules* **24**, (2019).

64. Terzuoli, E., Giachetti, A., Ziche, M. & Donnini, S. Hydroxytyrosol, a product from olive oil, reduces colon cancer growth by enhancing epidermal growth factor receptor degradation. *Mol. Nutr. Food Res.* **60**, 519–529 (2016).

65. Fabiani, R. *et al.* Cancer chemoprevention by hydroxytyrosol isolated from virgin olive oil through G1 cell cycle arrest and apoptosis. *Eur. J. Cancer Prev.* **11**, 351–358 (2002).

66. Serra, A. T. *et al.* The Journal of Supercritical Fluids Processing cherries (Prunus avium) using supercritical fluid technology . Part 1 : Recovery of extract fractions rich in bioactive compounds. *J. Supercrit. Fluids* **55**, 184–191 (2010).

67. Sambuy, Y. *et al.* The Caco-2 cell line as a model of the intestinal barrier : influence of cell and culture-related factors on Caco-2 cell functional characteristics The Caco-2 cell line as a model of the intestinal barrier : in £ uence of cell and culture-related factors. *Cell Biol. Toxicol.* **21**, 1–26 (2005).

68. Santana, J. Targeting colorectal cancer cell proliferation by bioactive triterpenic compounds derived from olive tree and raspberries using a 3D cell model approach João Gonçalo Domingues Santana. (Instituto Superior Técnico, Universidade de Lisboa, 2018).

69. STEMCELL Technologies. ALDEFLUOR™ Kit Product Description.

70. QIAGEN. RNeasy 96 Kit - QIAGEN Online.

71. Tutino, V., Caruso, M. G., Messa, C., Perri, E. & Notarnicola, M. Antiproliferative, antioxidant and anti-inflammatory effects of hydroxytyrosol on human hepatoma HepG2 and Hep3B cell lines. *Anticancer Res.* **32**, 5371–5377 (2012).

72. Han, J., Talorete, T. P. N., Yamada, P. & Isoda, H. Anti-proliferative and apoptotic effects of oleuropein and hydroxytyrosol on human breast cancer MCF-7 cells. *Cytotechnology* **59**, 45–53 (2009).

73. Luo, C. *et al.* Hydroxytyrosol Promotes Superoxide Production and Defects in Autophagy Leading to Anti-proliferation and Apoptosis on Human Prostate Cancer Cells. *Curr. Cancer Drug Targets* **13**, 625–639 (2013).

74. Fabiani, R. *et al.* Anti-proliferative and pro-apoptotic activities of hydroxytyrosol on different tumour cells: The role of extracellular production of hydrogen peroxide. *Eur. J. Nutr.* **51**, 455–464 (2012).

75. Rodrigues, L. *et al.* Recovery of antioxidant and antiproliferative compounds from watercress using pressurized fluid extraction. *RSC Adv.* **6**, 30905–30918 (2016).

76. Turck, D. *et al.* Safety of hydroxytyrosol as a novel food pursuant to Regulation (EC) No 258/97. *EFSA J.* **15**, (2017).

77. FDA. *Determination of the Generally Recogniced As Safe (GRAS) Status of Hydroxytyrosol as a Food Ingredient*. (2015).

78. Fan, X., Ouyang, N., Teng, H. & Yao, H. Isolation and characterization of spheroid cells from the HT29 colon cancer cell line. *Int. J. Colorectal Dis.* **26**, 1279–1285 (2011).

79. Lee, S.-H. *et al.* Colorectal cancer-derived tumor spheroids retain the characteristics of original tumors. *Cancer Lett.* **367**, 34–42 (2015).

80. Jelski, W. & Szmitkowski, M. Alcohol dehydrogenase (ADH) and aldehyde dehydrogenase (ALDH) in the cancer diseases. *Clin. Chim. Acta* **395**, 1–5 (2008).

81. Cruz-Lozano, M. *et al.* Hydroxytyrosol inhibits cancer stem cells and the metastatic capacity of triple-negative breast cancer cell lines by the simultaneous targeting of epithelial-to-mesenchymal transition, Wnt/β-catenin and TGFβ signaling pathways. *Eur. J. Nutr.* **0**, 0 (2018).

82. Corominas-Faja, B. *et al.* Extra-virgin olive oil contains a metabolo-epigenetic inhibitor of cancer stem cells. *Oxford Univ. Press.* (2018). doi:10.1093/neuonc/noy094/5025434

83. Borowicz, S. *et al.* The soft agar colony formation assay. *J. Vis. Exp.* 1–6 (2014). doi:10.3791/51998

84. Taddei, M. L., Giannoni, E., Fiaschi, T. & Chiarugi, P. Anoikis: An emerging hallmark in health and diseases. *J. Pathol.* **226**, 380–393 (2012).

85. Guadamillas, M. C., Cerezo, A. & del Pozo, M. A. Overcoming anoikis - pathways to anchorageindependent growth in cancer. *J. Cell Sci.* **124**, 3189–3197 (2011).

86. Ricci-Vitiani, L. *et al.* Identification and expansion of human colon-cancer-initiating cells. *Nature* **445**, 111–115 (2007).

87. Terzuoli, E. *et al.* Inhibition of cell cycle progression by the hydroxytyrosol- cetuximab combination yields enhanced chemotherapeutic efficacy in colon cancer cells. *Oncotarget* **8**, 83207–83224 (2017).

88. Baselga, J. The EGFR as a target for anticancer therapy - Focus on cetuximab. *Eur. J. Cancer* **37**, 16–22 (2001).

89. Bernini, R. *et al.* Synthesis of a novel ester of hydroxytyrosol and α-lipoic acid exhibiting an antiproliferative effect on human colon cancer HT-29 cells. *Eur. J. Med. Chem.* **46**, 439–446 (2011).

90. Srimuangwong, K., Tocharus, C., Chintana, P. Y., Suksamrarn, A. & Tocharus, J. Hexahydrocurcumin enhances inhibitory effect of 5-fluorouracil on HT-29 human colon cancer cells. *World J. Gastroenterol.* **18**, 2383–2389 (2012).

91. Fantini, M. *et al.* In vitro and in vivo antitumoral effects of combinations of polyphenols, or polyphenols and anticancer drugs: Perspectives on cancer treatment. *Int. J. Mol. Sci.* **16**, 9236–9282 (2015).

92. Rafehi, H. *et al.* Investigation into the biological properties of the olive polyphenol, hydroxytyrosol: Mechanistic insights by genome-wide mRNA-Seq analysis. *Genes Nutr.* **7**, 343–355 (2012).

93. Tejal Patel, MD, T. M. H. S. Olive Oil for High Risk Breast Cancer Prevention in Women. *Clinical Trials* Available at: https://clinicaltrials.gov/ct2/show/NCT02068092?cond=hydroxytyrosol&draw=2&rank=8. (Accessed: 3rd November 2019)

94. Hu, T., He, X. W., Jiang, J. G. & Xu, X. L. Hydroxytyrosol and its potential therapeutic effects. *J. Agric. Food Chem.* **62**, 1449–1455 (2014).

95. González-Santiago, M., Fonollá, J. & Lopez-Huertas, E. Human absorption of a supplement containing purified hydroxytyrosol, a natural antioxidant from olive oil, and evidence for its transient association with low-density lipoproteins. *Pharmacol. Res.* **61**, 364–370 (2010).